



URNAL OF
BUILDING
MATERIAL SCIENCE

VOLUME 1 ISSUE 1 · APRIL 2019

ISSN: 2630-5216 (ONLINE)

BILINGUAL PUBLISHING Co.

Editor-in-Chief

Huang Ying North Dakota State University, United States



**BILINGUAL
PUBLISHING CO.**
Pioneer of Global Academics Since 1984

Editorial Board Members

Suman Saha	National Institute of Technology, India
Guo Meng	Beijing University of Technology, China
Zhang Ning	North China Electric Power University, China
Rui Duarte Neves	Polytechnic Institute of Setubal, Portugal
Liu Quantao	Wuhan University of Technology, China
Susana Hormigos-Jimenez	San Pablo CEU University, Spain
Pavel Krivenko	Kyiv National University of Construction and Architecture, Ukraine
Ehsan Ghafari	Purdue University, United States
Bai Chengying	University of Padova, Italy
Santiranjana Shannigrahi	Institute of Materials Research and Engineering (ASTAR), Singapore
Mohammad Reza Tohidifar	University of Zanjan, Iran
Bharat Bhushan Jindal	Maharishi Markandeshwar University, Ambala, India
Gamal Abou-Elgheat Khater	National Research Centre, Egypt
Mohammad Heydari Vini	Islamic Azad University, Iran
Du Shiyu Ningbo	Institute of Materials Technology & Engineering, China
Morteza Tayebi	Islamic Azad University, Iran
Hong Changqing	Harbin Institute of Technology, China
Zahra Abdollahnejad	Oulu University, Finland
Hadel Ibraheem Ahmad Obaidi	Middle Technical University, Iraq
Ahmed S. H.	Suwaed Heriot-Watt University, United Kingdom
Chen Yang	Northeastern University, China
Luigi Coppola	University of Bergamo, Italy
Han Jian-Yong	Northeastern University, China
Qin Ying	Southeast University, China
Shu Biao	Central South University, China
Zhang Hongliang	Chang'an University, China
Wang Huaping	Lanzhou University, China
Ma Qinglin	Shandong University, China
Abdelkader Bougara	University Center Hassiba Benbouali, Algeria
Kien Ngoc Bui	Thuyloi University, Vietnam
Shi Xijun	Texas A&M University, United States
Rawaz M. S. Kurda	University of Lisbon - Instituto Superior Técnico, Portugal
Zahra Pezeshki	Shahrood University of Technology, Iran
Kiran Devi	National Institute of Technology, Kurukshetra, India
Mustafa Eken	Kahramanmaraş Istiklal University, Turkey
Mahmood Md Tahir	Universiti Teknologi Malaysia, Malaysia
Feng Huihong	Southwest Petroleum University, China
Tulio Hallak Panzera	Federal University of São João del Rei – UFSJ, Brazil
Lu Xiaoshu	University of Vaasa, Finland
Jacopo Donnini	Marche Polytechnic University, Italy
Hosam El-Din Mostafa Saleh	Egyptian Atomic Energy Authority, Egypt
Rohola Rahnavard	Clarkson University, United States
Subash Chandra Mishra	National Institute of Technology, Rourkela, India
Ranjana Jha	Netaji Subhas University of Technology, India
Ali Tighnavard Balasbaneh	Universiti Teknologi Malaysia, Malaysia
Leila Soufeiani	University of Melbourne, Australia
Sudarshan Dattatraya Kore	National Institute of Construction Management and Research (NICMAR), India
Wang Song	Georgia Southern University, United States

Reviewers

Christophe Delebarre	University of Valenciennes, France
Soumya Mukherjee	Amity University, Kolkata, India

Volume 1 Issue 1 June 2019 ISSN 2630-5216 (Online)

JOURNAL OF BUILDING MATERIAL SCIENCE

Editor-in-Chief

Huang Ying

North Dakota State University, United States



**BILINGUAL
PUBLISHING CO.**

Pioneer of Global Academics Since 1984

Contents

Article

- 1 Steatite/Epoxy Composites for Restoration Works Through a Statistical Mixture Design Methodology**
Robinson Antonio Aparecido Alves, Julio Cesar dos Santos, Kurt Strecker, Tulio Hallak Panzera, Robson Bruno Dutra Pereira
- 10 Retrofitting Steel Moment Frames by Using the Cable Bracing**
Mohammad Naghavi
- 18 A Numerical Study of the Behavior of Steel Frame with Concentric Buckling Restrained and Conventional Braces**
Mohammad Naghavi, Mohsen Malekinejad
- 26 Feasibility Study on Use of Plastic Waste as Fine Aggregate in Concrete Mixes**
Sudarshan Dattatraya Kore
- 32 Significance of Stone Waste in Strength Improvement of Soil**
Amit Kumar, Kiran Devi, Maninder Singh, Dharmender Kumar Soni

Copyright

Journal of Building Material Science is licensed under a Creative Commons-Non-Commercial 4.0 International Copyright (CC BY- NC4.0). Readers shall have the right to copy and distribute articles in this journal in any form in any medium, and may also modify, convert or create on the basis of articles. In sharing and using articles in this journal, the user must indicate the author and source, and mark the changes made in articles. Copyright © BILINGUAL PUBLISHING CO. All Rights Reserved.

ARTICLE

Steatite/Epoxy Composites for Restoration Works Through a Statistical Mixture Design Methodology

Robinson Antonio Aparecido Alves¹ Julio Cesar dos Santos¹ Kurt Strecker¹

Tulio Hallak Panzera^{1*} Robson Bruno Dutra Pereira¹

1. Centre for Innovation and Technology in Composite Materials (CITeC), Department of Mechanical Engineering, Federal University of São João del Rei (UFSJ), 36307352, Brazil

ARTICLE INFO

Article history

Received: 18th February 2019

Accepted: 29th April 2019

Published: 29th April 2019

Keywords:

Planning of experiments

Composites

Restoration

Steatite

ABSTRACT

Currently many works of art made of soapstone and recognised as cultural patrimony of humanity are in an advanced stage of degradation. Hence, it is necessary to interrupt this process and recover the deteriorated parts. Composite materials consisted of steatite particles and epoxy polymer are designed and characterised for their application in the repair of sculptures made of soapstone. The material applied in restorations should provide colouration and texture similar to soapstone besides structural requirements. The degree of similarity of the artificial material to the rock is enhanced by the proper selection of the particle size range and the increase of the weight percent of steatite incorporated in the composites. A statistical methodology based on the mixture design is used to optimise the relative amount of three size of steatite particles in order to maximise the weight percent of dispersed phase in the composites. The maximum particle packing density (1.50 g/cm³) is obtained for a ternary mixture, composed of 62 wt.% of coarse particles (1.18 mm - 0.60 mm), 6 wt.% of medium sized particles (0.60 mm - 0.30 mm) and 32 wt.% of fine particles (0.30 mm - 0.15 mm). In this manner, the fabrication of composites based on an epoxy polymer matrix with 70 wt.% of incorporated steatite particles has been possible, increasing the maximum amount by 10 % as used in previous works.

1. Introduction

The technique of rock carving has been used in the constructions of Brazil since the 16th century, reaching its apex and primarily in the state of Minas Gerais during the 18th century. In this region, the art was implanted by influence of the Portuguese and acquired local peculiarities thanks to the creativity of the native artists. These artists dominated the eighteenth-

century architecture and helped to compose the beautiful and original collection that characterises the baroque style of Minas Gerais^[1]. During the eighteenth century many cities in the Brazilian's country side were founded because of the discovery of large gold deposits. The hope for prosperity and enrichment brought by the precious metal attracted large numbers of migrants and resulted in a strong economic development of these regions. Population

*Corresponding Author:

Tulio Hallak Panzera,

Centre for Innovation and Technology in Composite Materials (CITeC), Department of Mechanical Engineering, Federal University of São João del Rei (UFSJ), 36307352, Brazil

Email: panzera@ufsj.edu.br

growth and abundant financial resources boosted the local economy. These factors, allied to the strong religious tradition of that time in Brazil, resulted in the construction of magnificent churches with ornate facades and countless works of art^[2].

In this prosperous scenario, great artists of the baroque appeared; Antonio Francisco Lisboa, popularly known as Aleijadinho, being the most famous. Like Aleijadinho, many sculptors of that time used blocks of rock as the main raw material for the manufacture of sculptures and ornaments of churches. Steatite, also known as soapstone, was the favourite rock material used by these sculptors, because of its low hardness, and, therefore, the great ease of obtaining precise and delicate details of the artefacts. However, this striking feature also turns soapstone susceptible to wear and, unfortunately, to acts of vandalism. Many artefacts made of soapstone, considered as cultural patrimony of humanity, are currently in an advanced stage of degradation^[3]. Therefore, it is necessary to develop techniques and actions for the maintenance and restoration of these artefacts. In view of this need, this work aimed to develop suitable composite materials for application in the repair of superficial wear, replacement of damaged parts and production of replicas of sculptures in soapstone.

In this way, studies have been conducted on developing suitable materials to be used in the restoration of artefacts made from soapstone. The material used in such restorations must present, as one of their main characteristic, colouration and texture similar to the original stone, and acceptable structural properties. Therefore, composites made with different weight percent of particles of soapstone itself and different weight percent of binders have been studied in order to obtain a material suitable for restoration works^{[4][5][6]}.

Strecker et al.^[4] have investigated the effect of adding steatite residues in different grain sizes on the mechanical properties of cementitious composites. Panzera et al.^[5] have developed hybrid composites, for restoration works, made of Portland cement, steatite particles and unidirectional carbon fibres, aiming to increase the flexural strength of the material. Cota et al.^[6] have studied the mechanical behaviour of composites manufactured with steatite residues and matrices consisting of mixtures of epoxy polymer and Portland cement paste in different proportions. The maximum amount of steatite particles added by these researchers was 60 wt.%. The main difficulties encountered were the low workability and the low capacity of material densification and the loss of mechanical strength, which have been the main limiting factors for an increase of the weight percent of dispersed

phase in these composites.

A small number of studies have been carried out with the aim of developing and characterising materials for restoration of historical monuments manufactured with other types of rock. Torney et al.^[7] developed a study in order to compare some physical properties of the sandstone with the properties of two types of commercial mortars applied in restoration of rocks. Stefanidou et al.^[8] have studied the development of mortar for application in restoration of monuments manufactured with different types of rock. The authors carried out a study to investigate the colour ratio of the mortars according to the aggregate used. It has been found that a correct selection of the type, size and weight fraction of the aggregate can generate artificial materials with colouration and texture similar to natural rock. Particle size and the weight percent of steatite particles incorporated into the composites are the main factors associated with the degree of physical similarity between the artificial material and the rock. Therefore, in order to produce materials with colour and texture similar to soapstone, a high weight percent of dispersed phase in the composite material is desired. This can be achieved by maximising the packing density of steatite particles, a factor that also contributes to increased mechanical strength of the material^[9]. Particle packing is the problem of the correct selection of proportions and sizes of the particulate materials. The highest particle packing is obtained when large voids are filled with small particles whose voids are again filled with even smaller particles and so on^[10].

Particle packing can be represented quantitatively by the packing density, defined as the mass of solid in a unit of total volume. The materials with high packing density have low volume of voids between particles and, consequently, require a smaller weight percent of binding material as matrix. Various properties of particulate composites are related to the packing of particles representing the dispersed phase. High packing densities are fundamental to obtain particulate composites of low porosity and, in consequence, with enhanced mechanical properties^[11].

The particle size distribution of the system or the filling sequence of the voids between the particles determines whether a high packing density is achieved. Therefore, it is important to optimise the relative amounts of different sized particle fractions that constitute the system^[12]. This optimisation can be performed by the use of a statistical methodology based on mixture design experiments. Experiments with mixtures are those where two or more ingredients are mixed to form a product. The response of interest to be measured constitutes a property of

the mixture, depending only on the proportions of the components present (whether in mass, volume or molar ratio), and not on the total amount of the mixture. A general objective of this experimental design is the modelling and analysis of the response surface of the mixture. This methodology is based on a limited number of observations considering pre-selected proportions of the components, resulting in mixtures of different compositions^[13]. By modelling the surface of response of the mixtures it is possible to obtain a prediction of the response for any composition of the mixture within the region covered by the experiment, and consequently, to estimate the optimum composition of the studied mixture^[14].

This work aims to maximise the packing density of steatite particles in order to increase the weight percent of dispersed phase incorporated in composites destined to the restoration of artefacts made of soapstone. This was achieved by optimising the particle size distribution using a statistical methodology based on the planning of three component mixture experiment.

2. Materials and Methods

An epoxy polymer is used as matrix phase, while particles of soapstone are used as dispersed phase.

2.1 Matrix Phase: Epoxy Resin Polymer

A liquid epoxy resin based on bisphenol A, LY-1316 2BR, and Aradur 2963 curing agent, based on cycloaliphatic amines, are used as matrix material for the investigated composites. This set of resin and hardener are produced by the Huntsman Company (Brazil). The recommended ratio between resin and hardener, as well as some other properties, are provided by the manufacturer, as shown in Table 1.

Table 1. Properties of Araldite LY – 1316 2BR and Hardener Aradur 2963 and the Mixture Thereof (Source: Huntsman Ltd.)

Characteristics	Product	Data
Proportion of mixture (in mass)	Resin	100g
	Hardener	48g
Density at 25°C	Resin	1.0 a 1.05 g/cm ³
	Hardener	1.0 g/cm ³
	Mixture	1.0 to 1.05 g/cm ³

Viscosity at 25°C	Resin	1000 - 1200 mPas
	Hardener	30 – 70 mPas
	Mixture	300 – 400 mPas
Time of use at 25°C	Mixture	35 minutes
Time for demoulding at 25°C	Mixture	8 to 10 hours
Curing time at 25°C	Mixture	7 days

This epoxy system (LY – 1316 2BR/2963) was chosen due to its relatively low viscosity and the combination of suitable properties for the composite manufacturing process. This characteristic is fundamental to ensure a high physical adhesion upon porous surfaces and a high percentage of the dispersed phase (steatite particles) without compromising the workability of the material. Moreover, LY - 1316 2BR/2963 epoxy polymer also provides a combination of important and desirable characteristics for restoration applications such as colourlessness. This set also provides a system for easy handling and curing at room temperature. According to the manufacturer, the final product after curing is rigid and presents an excellent balance between its mechanical, thermal and chemical resistance, associated with low contraction, high adhesion, high cohesion and optimum dimensional stability.

2.2 Dispersed Phase: Steatite Particles

The steatite particles were collected from a local manufacturer of pans and artefacts of soapstone, located in the city of Congonhas (Brazil). The steatite residues were dried in an oven at 110°C for 24 hours. The chemical analysis of the soapstone residue was obtained by X-ray fluorescence spectrometry as shown in Table 2. The high content of silicon oxide (44.78 %) and magnesium oxide (29.24 %) found in the soapstone powder is characteristic of the mineral talc, the main constituent of steatite^[15].

Table 2. Composition of Steatite residue.

Compound	Quantity (%)
SiO ₂	44.78
Al ₂ O ₃	3.65
Fe ₂ O ₃	8.34
TiO ₂	< 0.001
CaO	2.99
MgO	29.24
Na ₂ O	< 0.001
K ₂ O	< 0.001
MnO	0.15
P ₂ O ₅	0.01
Loss on ignition	10.36

Table 3. Particle size analysis of the steatite residue.

PARTICLE SIZE DISTRIBUTION - STEATITE (300g)								
SIEVE		SAMPLE 1		SAMPLE 2		% Mean		
ASTM E11-17 [18]	Opening (mm)	Retained mass (g)	% Retained	Retained mass (g)	% Retained	Retained	Cumulative percent retained	Cumulative percent passing
3"	75.00	0.00	0.00	0.00	0.00	0.00	0.00	100.00
1.1/2"	37.50	0.00	0.00	0.00	0.00	0.00	0.00	100.00
3/4"	19.00	0.00	0.00	0.00	0.00	0.00	0.00	100.00
3/8"	9.50	0.00	0.00	0.00	0.00	0.00	0.00	100.00
4	4.75	5.17	1.73	5.37	1.79	1.76	1.76	98.24
8	2.36	22.10	7.38	22.80	7.61	7.50	9.26	90.74
16	1.18	47.20	15.77	47.07	15.72	15.74	25.00	75.00
30	0.60	72.59	24.25	71.79	23.97	24.11	49.10	50.90

50	0.30	48.74	16.28	48.08	16.05	16.17	65.27	34.73
100	0.15	32.82	10.96	31.53	10.53	10.74	76.01	23.99
PAN		70.77	23.64	72.88	24.33	23.99	100.00	0.00
TOTAL		299.39	100.00	299.52	100.00	100.00	226.40	

Fineness modulus: 2.26

Subsequently, the powders were characterised by its grain size distribution, as recommended by the standards ASTM C136M-14^[16] and NBR NM 248-03^[17]. An electromagnetic stirrer and a set of standard sieves^[18] were used to determine the grain size distribution of the steatite residue from the pans manufacturing process (Table 3).

The grain size distribution of the steatite residue is close to the limits established by standards NBR 7211-09^[19] and ASTM C144-11^[20] but does not fully comply with them. Therefore, to be used as fine aggregate in concretes and mortars, the soapstone residue must have its grain size distribution adjusted to suit the requirements provided by these standards. The grain size distribution curves are shown in Figure 1.

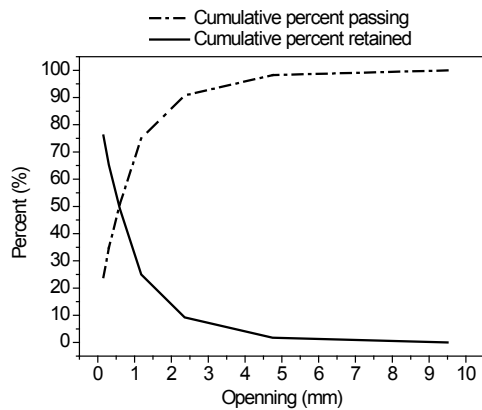


Figure 1. Particle Size Distribution of Steatite Residue

The particle size distribution curve presents a continuous behaviour in the size range between 4.75 mm and 0.15 mm. This behaviour indicates that the investigated steatite residue is well-graded and does not present discontinuities in the analysed range. Aggregates with a continuous particle size distribution favour higher particle packing densities^[21].

The particle size distribution of steatite used in this work is obtained following the recommendations of ASTM C136M-14^[16] and NBR NM 248-03^[17]. However, the grain size range for composite manufacturing is selected prioritising the best material suitability for restorations. Dense particle packing is fundamental to obtain particulate composites with low porosity and, consequently, materials with enhanced mechanical properties. Therefore, an effort is made to use an aggregate with a large and continuous particle size distribution, as these factors contribute positively to the increase of

the particle packing density^[21]. However, an upper limit and lower limit of particle size are established aiming at a better suitability of the material for its application in restoration works.

Composites produced with particles larger than 1.18 mm showed little penetration capacity into cracks, turning the material unsuitable for application in this type of defect^[9]. Composites made with particles smaller than 0.15 mm were also studied. These fine particles were lighter in colour than the natural stone. Consequently, the preliminary composites made of these particles exhibited a very different physical appearance as the rock^[9]. Therefore, the lower (0.15 mm) and upper (1.18 mm) limits of the steatite particle size was established. Within the established size range, the steatite is classified in monodisperse particles according to the standards NBR 7211-09^[19] and ASTM C144-11^[20]. These monodisperse particles are denominated coarse, medium and fine, as presented in Table 4 and in Figure 2.

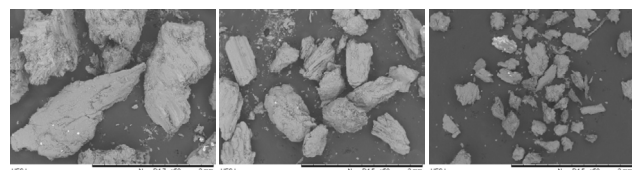
Table 4. Monodisperse Particle Levels of Steatite (ASTM E11-17^[18])

Particle Size	Sieve passing	Sieve retained
Coarse	16	30
Medium	30	50
Fine	50	100



Figure 2. Steatite Classified in Coarse, Medium and Fine Monodispersed Particles.

The characterisation of the steatite particle morphology was performed by scanning electron microscopy (SEM), Hitachi MEV-TM 3000, using backscattered electron mode (BSE) at 15 kV and carbon tape. Figure 3(a-c) shows the images of steatite particles at 50× of magnification.



(From Left) Figure 3. (a) Coarse (1.18 – 0.60 mm), (b) medium (0.60-0.30 mm) and (c) fine sized (0.30 – 0.15 mm) steatite particles.

The SEM images were compared with the standard NBR 7389-09^[22] to define the levels of sphericity and roundness of the particles. Through visual evaluation a great heterogeneity in the particle shape is identified, with particles of low sphericity and angular and subangular surfaces showing little evidence of wear. This morphology is characteristic of aggregates that undergo artificial comminution processes^[23], as is the case of the soapstone particles used in this work. This type of morphology presented by the soapstone particles contributes negatively to the packaging. The further away from the spherical and angular shape are the particles, the lower the packing density of a distribution containing them. This is due to friction effects between particles with irregular surfaces. The smaller the size of the irregular particles, the greater this effect will be, due to the greater specific surface area^[21].

2.3 Experimental Planning with Mixtures

In order to maximise the packing density of the steatite particles, the mixture design of experiment was used in this project. The simplex-centroid design for mixtures with three components was applied in the system consisting of coarse, medium and fine monodispersed particles. This model is represented by an equilateral triangle with seven points; the dots represent the different pre-selected compositions that are tested. In a three-component mixture, each experiment at the vertices represents the formulations of a pure component, while the centre of the edges of the equilateral triangle represents the binary mixtures and compositions within the triangle the ternary mixtures, as shown in Figure 4.

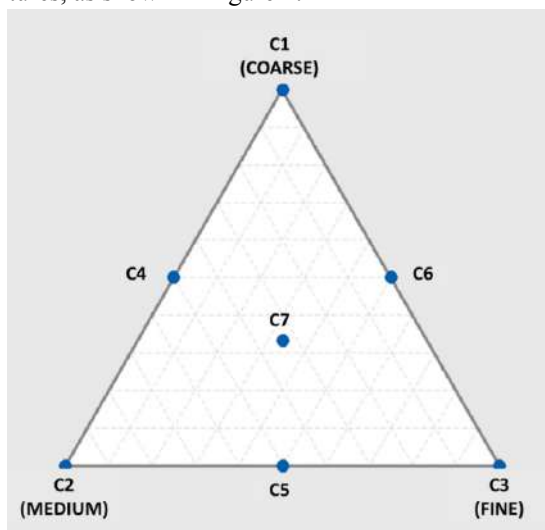


Figure 4. Simplex-centroid Surface for Three Distinct Particle Size Classes

The components of each composition were weighed and mixed to homogenise the material. Subsequently, one

at a time, the mixtures were placed in a graduated cylinder and subjected to vibration on an electromagnetic stirrer for three minutes. The packing density of each composition is calculated by dividing the mass of each mixture by the total volume occupied by the particles in the beaker after vibration. This procedure was performed for the seven different compositions and repeated twice, in order to minimise the experimental error of the results^[24]. The randomisation method was adopted during conduction of the tests, allowing an arbitrary ordering of the different compositions and avoiding that effects of uncontrolled factors could affect the response-variable^{[25][26]}.

The values obtained in the tests with pre-selected compositions were used to determine the coefficients (β) of the canonical polynomials of Scheffé and to generate the response surface (using Minitab software version 17, module "Mixture")^[27].

Two polynomial models applicable to the simplex-centroid design of three components ($q = 3$) were tested: quadratic model (Equation 1) and special cubic model (Equation 2).

$$\hat{y} = \beta_1 x_1 + \beta_2 x_2 + \beta_3 x_3 + \beta_{12} x_1 x_2 + \beta_{13} x_1 x_3 + \beta_{23} x_2 x_3 \quad (1)$$

$$\hat{y} = \beta_1 x_1 + \beta_2 x_2 + \beta_3 x_3 + \beta_{12} x_1 x_2 + \beta_{13} x_1 x_3 + \beta_{23} x_2 x_3 + \beta_{123} x_1 x_2 x_3 \quad (2)$$

On the equations 1 and 2, \hat{y} is the expected response for the proposed mixture, and x_1 , x_2 and x_3 represent the proportion of each of the three components of the mixture. The parameters $\beta_i x_i$ represent the expected response for the pure compositions. The terms $\beta_{ij} x_i x_j$ represent an alteration of the quadratic model response (degree two) over the linear model (degree one). The third-degree term $\beta_{ijk} x_i x_j x_k$ describes the response surface behaviour in the interior of the surface simplex^[28]. After the experimental packing tests, the polynomial model (R^2 and R^2 adjusted) that presented the best fit is chosen, and consequently, the best predictive capability for the response variable investigated.

The adjusted equation relates the packing density of the particles to the proportions of the three monodisperse particles used. By processing of the experimental data, a response surface was generated for the variable packing density. By means of the adjusted equation and the generated response surface it was possible to predict the behaviour of the response variable for different combinations of the monodisperse particles used. Thus, the packing density could be maximised by optimising the amounts of the three distinct monodisperse particles of different size ranges through non-linear programming.

2.4 Sample Preparation

Composite samples with the highest possible weight percent of dispersed phase were manufactured after the

optimisation of the amounts of the three monodisperse steatite particles, aiming at the development of a material with similar colour and texture as steatite rock. Based on previous studies^{[4][5][6]} and preliminary tests, composites were produced using three different weight percent of matrix phase (35 wt.%, 30 wt.% and 25 wt.%) and dispersed phase (65 wt.%, 70 wt.% and 75 wt.%).

The composites were manufactured by manually mixing 100 parts by mass of resin and 48 parts by weight of hardener for a period of 3 minutes, following the manufacturer’s recommendations. After homogenisation of the resin with the hardener, the polymer phase was manually mixed with the steatite particles in the different proportions over a period of 3 minutes. The materials were cast in silicone moulds and subjected to vibration in an electromagnetic stirrer for material accommodation and elimination of air bubbles entrapped. A mould with cylindrical shapes with dimensions recommended by ASTM D695-10^[29] is shown in Figure 5.

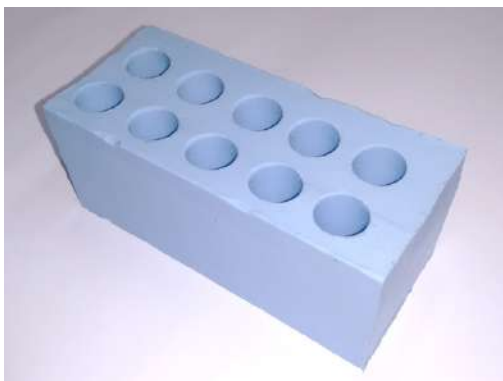


Figure 5. Silicon Mould Used to Manufacture Sample

After 48 hours the specimens of 40 mm height and 20 mm diameter were removed from the mould, identified and packed in a sealed plastic container. Curing of the specimens was performed at room temperature for a period of 7 days. Ten specimens from each of the three compositions were fabricated in a randomised order. In total, 30 specimens were produced, as recommended by ASTM D695-10^[29].

3. Results

The simplex-centroid design for mixtures with three components was applied to the system consisting of coarse, medium and fine monodisperse particles. The packing densities of the seven pre-selected mixtures by the simplex-centroid design are shown in Table 5.

Table 5. Packing Density of the Pre-selected Mixtures of Steatite Particles

Compositions	Packing density (g/cm ³)			
	R1	R2	Mean	Standard deviation
C1	1.420	1.429	1.425	0.006
C2	1.337	1.351	1.344	0.010
C3	1.238	1.225	1.232	0.009

C4	1.453	1.471	1.462	0.012
C5	1.488	1.479	1.484	0.006
C6	1.374	1.359	1.366	0.011
C7	1.471	1.479	1.475	0.006

The values obtained in the tests with pre-selected mixtures were used to determine the coefficients of the canonical polynomials of Scheffé and to generate the response surface for the variable packing density (using Minitab software version 17, module “Mixture”). Two polynomial models applicable to the three-component simplex-centroid delineation (q = 3) were tested, the quadratic model (Equation 1) and the special cubic model (Equation 2).

The quadratic model was chosen because it presented a better adjustment capacity to the experimental data (R² = 99.44 % and R² adjusted = 99.10 %). The adjusted R² and R² values close to 100 % indicate that the quality of the fit of the model is satisfactory. The adequacy of the statistical model used is verified through the normal probability plot for the residues presented in Figure 6. The behaviour of the residuals for the response variable packaging density of steatite particles was adequate for normal distribution conditions. The points are located approximately along a straight line and there are no outliers, which are points distant from the line and may represent a source of error in the data collection.

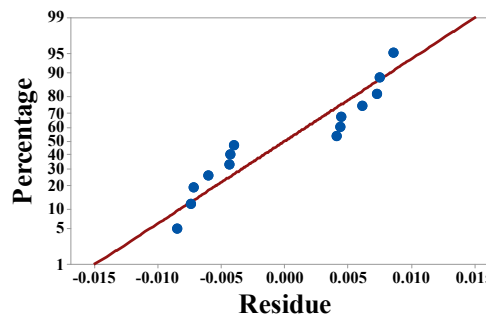


Figure 6. Normal Residual Probability Plot for the Packing Density of Steatite Particles

After the definition of the polynomial model and the verification of the adequacy of the model, the coefficients obtained through the statistical planning and the experimental data were inserted in Equation 1. The quadratic polynomial adjusted to the experimental data of packaging density of the steatite particles is presented in Equation 3.

$$\hat{y} = 1.42x_1 + 1.34x_2 + 1.23x_3 + 0.31x_1x_2 + 0.63x_1x_3 + 0.32x_2x_3 \quad (3)$$

Equation 3 relates the variable response packing density of the particles (\hat{y}) with the proportions of the monodisperse coarse (x_1), medium (x_2) and fine (x_3) particles used. By adjustment of the equation to the

experimental data it is possible to predict the behaviour of the variable response for all different combinations of the monodisperse mixtures. Consequently, it was possible to maximise the packing density of the particles by optimising the particle size distribution in the range investigated. The theoretical proportions of monodisperse particles for maximum packing density were obtained by maximising Equation 3.

The maximum particle packing density was obtained for a ternary mixture, composed of 62% of coarse particles (1.18 mm - 0.60 mm), 6% of medium sized particles (0.60 mm - 0.30 mm) and 32% of fine particles (0.30 mm - 0.15 mm). Inserting the values of the proportions in Equation 3, a theoretical packing density of 1.50 g/cm³ was obtained. This value was verified and confirmed by performing new experimental tests using the statistical modelling data.

Through experimental design with mixtures it was also possible to generate a contour plot for the behaviour of the variable packing density for all different combinations of proportions of the coarse, medium and fine monodisperse particles, see Figure 7.

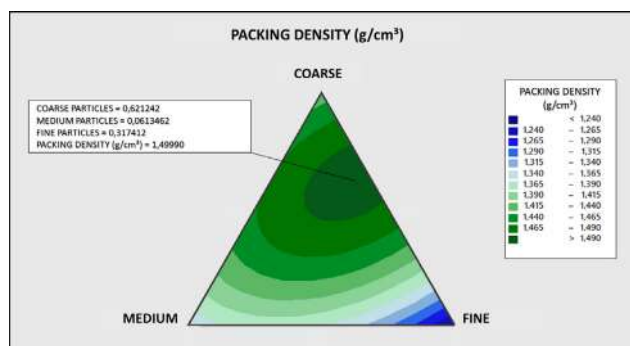


Figure 7. Contour Plot for the Variable Packing Density

Based on the contour plot it is possible to estimate the region of the experimental space which maximises packing density response of the steatite particles. As shown in Figure 7, the coarse monodispersed particles presented a higher packing density compared to medium and fine monodisperse particles, however, the region of the experimental space that presents the highest packing density is a ternary mixture composed of coarse, medium and fine particles. These findings confirm the theories reported in previous work^[21], assuming that larger irregular particles with a continuous particle size distribution produces denser packages.

After the optimisation of the size distribution of the steatite particles, composites were fabricated using an epoxy polymer (Table 1) as matrix and different weight percent of dispersed phase (65 wt.%, 70 wt.% and 75 wt.%) with the optimised grain size distribution.

In the attempt to develop a material with aesthetic

characteristics similar to those presented by soapstone, the largest possible weight percent of dispersed phase was incorporated to the composites. Therefore, based on previous studies^{[4][5][6]} and preliminary tests, composites with 25 wt.% of epoxy polymer and 75 wt.% of steatite particles were manufactured. However, this material presented very low fluidity, compromising the workability and the capacity of densification, leading to a large amount of external macro pores (Figure 8), especially for a cylindrical sample that makes it difficult to remove trapped air through its longitudinal length.

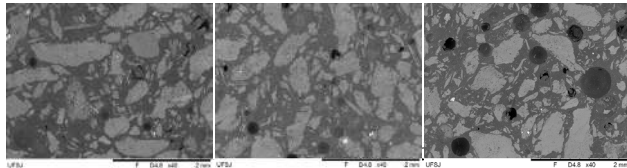
Due to the low fluidity of these composites, which resulted in high porosity, the weight percent of polymer matrix was increased, and the weight percent of steatite particles decreased. Thus, composites were fabricated with 70 wt.% and 65 wt.% of steatite particles. Contrary to the first percentage used, the mixture composed of 30 wt.% epoxy polymer and 70 wt.% of steatite particles revealed better workability and higher density with reduced amount and size of external macro pores. The blend consisting of 35 wt.% epoxy polymer and 65 wt.% steatite particles also showed adequate workability and density. However, this higher percentage of epoxy polymer (35 wt.%) was excessive and caused segregation of the steatite particles. The dispersed phase accumulated predominantly in the lower part of the specimens, generating a heterogeneous material along the longitudinal section (Figure 8).



Figure 8. Polymer-based Composites with 65 wt.%, 70 wt.% and 75 wt.% of Steatite Inclusions

The Hitachi MEV-TM 3000 Scanning Electron Microscope operating with backscattered electron mode at 15kV was used for the microstructural analysis of the composites. Figure 9 shows the composite images containing 65 wt.% (a), 70 wt.% (b) and 75 wt.% (c) of steatite particles with a 40 × magnification. Composites made with a large amount of steatite particles reveal the presence of a larger amount of macro pores (Figure 9c),

which can be attributed to the different rheology of the system that can affect the removal of internal bubbles. A good interface condition between the steatite particles and the matrix phase is evidenced even for the inclusion of large amounts of particles (75 wt.%), without pore formation or discontinuity.



65 wt.% (a), 70 wt.% (b) and 75 wt.% (c) of Steatite Particles

Table 6 shows bulk density values for the soapstone (natural stone) and composite materials. The bulk density of the composites ranged from 1.753 g/cm³ to 1.828 g/cm³. The composites obtained lower bulk density in relation to the natural soap stone due to the low-density polymer matrix (1.05 g/cm³, Table 1). The composites made with 30 wt.% of polymer and 70 wt.% of dispersed phase reached the highest mean bulk density due to their lower amount of matrix phase and internal pores. In addition, composites made with 30 wt.% of polymer matrix and 70 wt.% of steatite particles also exhibited colouration and texture very similar to natural rock as shown in Figure 10.

Table 6. Bulk Density of Natural Steatite Rock and Composite Materials

Compositions	Bulk density (g/cm ³)	
	Mean	Standard deviation
Steatite (soapstone)	2.884	0.005
C1 (35 wt.% of polymer and 65 wt.% of steatite)	1.753	0.009
C2 (30 wt.% of polymer and 70 wt.% of steatite)	1.828	0.007
C3 (25 wt.% of polymer and 75 wt.% of steatite)	1.802	0.011

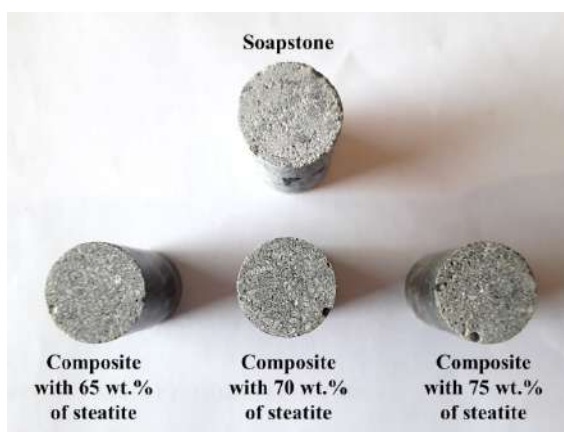


Figure 10. Aesthetic Characteristics of Soapstone and Composite Materials

Finally, composites made with 30 wt.% of polymer matrix and 70 wt.% of dispersed phase reached the most suitable properties and aesthetic characteristics for the

restoration of soapstone structures. In previous works^{[4][5][6]}, the maximum weight percentage of steatite particles in composites for restoration proposal was 60 wt.%.

4. Conclusion

The statistical methodology based on the three-component mixture experiment was used to optimise the particle size distribution of steatite particles. By means of this technique, the packing density of the steatite particles was maximised (1.50 g/cm³) by the optimisation of the size distribution within the investigated range. The optimised distribution allowed the production of composites with 70 wt.% of dispersed phase, 10% higher than the highest percentage used in previous works. This high percentage of weight contributes positively to the development of materials destined to the restoration of soapstone structures, with aesthetic characteristics similar to those of rock.

Acknowledgements

The authors would like to thank the Brazilian Research Agencies, CNPq (PP & PDE-205255/2017-5) and FAPEMIG (PPM-00075-17) and CAPES (MSc scholarship), for the financial support provided.

References

- [1] Stellin Junior, A. M. Mármore e granitos brasileiros. In: Congresso Brasileiro de Engenharia de Minas, 1990, Cagliari. Anais do Congresso Brasileiro de Engenharia de Minas, 1990.
- [2] Silva, M. E. Avaliação da susceptibilidade de rochas ornamentais e de revestimentos à deterioração: um enfoque a partir do estudo em monumentos do barroco mineiro. PhD Thesis, Instituto de Geociências da Universidade Federal de Minas Gerais. Belo Horizonte, 2007.
- [3] Silva, M. E., & Roeser, H. M. P. Mapeamento de deteriorações em monumentos históricos de pedra-sabão em Ouro Preto. Revista Brasileira de Geociências, v. 33, n. 4, p. 331-338, 2003. <https://doi.org/10.25249/0375-7536.2003334329336>.
- [4] Strecker, K., Panzera, T. H. & Sabariz, A. L. R. The effect of incorporation of steatite wastes on the mechanical properties of cementitious composites. Materials and Structures, v. 43, p. 923-932, 2010. <https://doi.org/10.1617/s11527-009-9556-1>.
- [5] Panzera, T. H., Strecker, K., Miranda, J. S., Christoforo, A. L., & Borges, P. H. R. Cement – Steatite Composites Reinforced with Carbon Fibres: an Alternative for Restoration of Brazilian Historical Buildings. Materials Research, v. 14, p. 118-123, 2011. <http://dx.doi.org/10.1590/S1516-14392011005000007>

- [6] Cota, F. P., Alves, R. A. A., Panzera, T. H., Strecker, K., Christoforo, A. L., & Borges, P. H. R. Physical properties and microstructure of ceramic-polymer composites for restoration works. *Materials Science and Engineering A*, v. 531, p. 28-34, 2012. <https://doi.org/10.1016/j.msea.2011.10.003>
- [7] Torney, C., Forster, A. M., & Szadurski, E. M. Specialist 'restoration mortars' for stone elements: a comparison of the physical properties of two stone repair materials. *Heritage Science*, 2014 2:1. <https://doi.org/10.1186/2050-7445-2-1>
- [8] Stefanidou, M., Vasiliki, P., & Papayianni, I. Design and testing of artificial stone for the restoration of stone elements in monuments and historic buildings. *Construction and Building Materials*, v. 93, p. 957-965, 2015. <https://doi.org/10.1016/j.conbuildmat.2015.05.063>
- [9] Alves, R. A. A. Desenvolvimento e caracterização de compósitos cerâmicos e cerâmico-poliméricos destinados a restauração de monumentos históricos fabricados em esteatito (pedra-sabão). MSc Thesis, Programa de pós-graduação em engenharia mecânica da Universidade Federal de São João Del Rei. São João Del Rei, 2017. Available at: <https://ufsj.edu.br/portal2-repositorio/File/ppmec/Dissertacao%202017-Robinson%20Alves.pdf>
- [10] McGeary, R. K. Mechanical packing of spherical particles. *Journal of the American Ceramic Society*, v. 44, n. 10, p. 513-522, 1961. <https://doi.org/10.1111/j.1151-2916.1961.tb13716.x>
- [11] Mehta, P. K., & Monteiro, P. J. M. *Concrete: Microstructure, Properties and Materials*. 3. ed. United States of America: McGraw-Hill Companies, 2006.
- [12] Conceicao, E. S. Influência da distribuição granulométrica no empacotamento de matérias-primas na formulação de porcelânicos. MSc Thesis, Escola Politécnica da Universidade de São Paulo. São Paulo, 2011.
- [13] Nunes, D. B. Rotinas para a otimização experimental de misturas. MSc Thesis, Programa de pós-graduação em engenharia de produção da Universidade Federal do Rio Grande do Sul. Porto Alegre, 1998.
- [14] Cornell, J. A. *Experiments with mixtures: Designs, Models, and the Analysis of Mixture data*. 3. ed. New York: John Wiley & Sons, 2002.
- [15] Pinheiro, J. C. F. *Perfil Analítico do Talco*. Rio de Janeiro: DNPM, 1973.
- [16] American Society for Testing and Materials. ASTM C136M-14: Standard Test Method for Sieve Analysis of Fine and Coarse Aggregates, 2014.
- [17] Associação Brasileira de Normas Técnicas. NBR NM 248: Agregados - Determinação da composição granulométrica, Rio de Janeiro, 2003.
- [18] American Society for Testing and Materials. ASTM E11-17: Standard Specification for Woven Wire Test Sieve Cloth and Test Sieves, 2017.
- [19] Associação Brasileira de Normas Técnicas. NBR 7211: Agregados para concreto - Especificação, Rio de Janeiro, 2009.
- [20] American Society for Testing and Materials. ASTM C144-11: Standard Specification for Aggregate for Masonry Mortar, 2011.
- [21] Oliveira, F. R., Studart, A. R., Pileggi, R. G., Pandolfelli, V. C. De Oliveira, R. C., de Oliveira, M. I. P., Studart, R., Pileggi, R. M., & Pan, V. *Dispersão e empacotamento de partículas-Princípios e aplicações em processamento cerâmico*. São Paulo: Fazendo Arte Editora, 2000.
- [22] Associação Brasileira de Normas Técnicas. NBR 7389: Apreciação petrográfica de materiais naturais, para utilização como agregado em concreto, Rio de Janeiro, 2009.
- [23] Neville, A. M. *Properties of concrete*. 5. ed. Harlow: Pearson Longman, 2011.
- [24] Panzera, T. H. Estudo do comportamento mecânico de um compósito particulado de matriz polimérica. MSc Thesis, Escola de engenharia da Universidade Federal de Minas Gerais. Belo Horizonte, 2003.
- [25] Button, S. T. *Metodologia para planejamento experimental e análise de resultados*. Campinas: UNICAMP, 2005.
- [26] Montgomery, D. C. *Design and Analysis of Experiments*, 8. ed. Cary: John Wiley & Sons, 2013.
- [27] Scheffe, H. Experiments with mixtures. *Journal of the Royal Statistical Society*, v. 20, p. 344-360, 1958. <https://www.jstor.org/stable/2983895>
- [28] Nepomucena, T. M. Análise da crista em experimentos de misturas com restrição na variância de predição. PhD Thesis, Programa de Pós-Graduação em Estatística e Experimentação Agropecuária da Universidade Federal de Lavras. Lavras, 2013.
- [29] American Society for Testing and Materials. ASTM D695-10: Standard Test Method for Compressive Properties of Rigid Plastics, 2010.

ARTICLE

Retrofitting Steel Moment Frames Using Cable Bracing

Mohammad Naghavi*

1. Department of Civil Engineering, Javid Institute for Higher Education of Jiroft, Iran

ARTICLE INFO

Article history

Received: 18th February 2019

Accepted: 29th April 2019

Published: 29th April 2019

Keywords:

Steel moment frames

Cable bracing

Nonlinear behavior

Hysteresis curve

ABSTRACT

In this paper, the behavior of retrofitted steel moment frames with bracing has been investigated. Braces include double-channel cross brace, cross braces with cable and brace with two cables passed through a cylindrical steel sheath at the location of the cables. Nonlinear analysis of frames has been carried out under cyclic loading with increasing amplitudes. Comparison of numerical analysis results with laboratory data shows the accuracy of finite element models. By determining the hysteresis and plasticity behavior of the frames, advantages and disadvantages of each of the retrofitting methods have been examined. The results have shown the use of double channels and cables to retrofit the frame increases the initial hardness and final load of the frame considerably compared to the moment frames and reduces its ductility. In frame with sheathed cable brace, the initial hardness was the same with the moment frames and the frame has been shown to have ductile behavior.

1. Introduction

Steel moment frames are designed in areas of high and very high seismic risk as well as medium to high ductility. These frames have sufficient ductility and amortization capacity with tolerance of great plastic deformities and rotations at the site of plastic hinges and fittings. Thus, the coefficient of behavior is considered to be large in the design of such frames and their design forces are less than other structural systems. Reinforcement of existing moment frames becomes necessary in cases such as unpredictable incidents, severe earthquakes or structural changes. Some researchers have tried to examine the retrofitting of moment frames using convergent and divergent braces^{[1][2][3][4][5]}. Other studies have been carried out to retrofit the steel frame using buckling restrained brace^{[6][7]} or a steel shear wall^[8]

^{[9][10]}. Some disadvantages are observed in conventional retrofitting methods for moment frames, by adding braces including increased axial force of pillars adjacent to braces because of the bracing operation and therefore the need for retrofitting the pillars and foundation, change of the ductile frame behavior to brittle behavior, buckling of the compressive member of brace and a permanent deformation are observed in the frame^{[11][12][13]}. In order to eliminate these disadvantages, some studies been done in which methods such as the use of non-pressure braces, buckling-resistant braces, and dissipating steel bracing have been examined in order to remove the possibility of buckling and maintain the frame ductility^[13]. The research seeks to find a way to simultaneously meet the goals outlined above. A method for retrofitting steel moment frames has been suggested using cable brace in which

*Corresponding Author:

Mohammad Naghavi,

Department of Civil Engineering, Javid Institute for Higher Education of Jiroft, Iran

Email: mn147013@gmail.com

two steel cables are passed through a cylindrical sheath at a point of impact. The bracing member does not come into action for low to moderate amplitude of vibrations. It controls the relative displacement for large amplitude of vibrations among the floors in a given range. Also, the frame behavior with a proposed bracing, moment frame without brace and curved frames with cross cables under cyclic loading have been experimentally investigated. In the present paper, the behavior of steel moment frames retrofitted with three types of bracing has been studied. To retrofit steel moment frames, three ways including use of cross brace with double-channels, cross brace with cables as well as brackets are examined with two cables passed through a cylindrical steel sheath at the junction of the cables. Finite element models of single moment frame as well as three retrofitted moment frames have been created using the ABAQUS software^[14].

Nonlinear behavior of steel materials nonlinear contact among cable components, brace and steel sheaths as well as nonlinear geometric formulation have been considered to predict rotating cylindrical sheath in finite element models. Moreover, nonlinear analysis of frames has been carried out under cyclic loading with increasing amplitudes. Comparison of results obtained from finite element analysis has been done with increasing amplitudes. Comparing finite element results with experimental data shows the accuracy of finite element models. For the examined frames, Force-displacement cyclic behavior, plasticity in frames and failure mechanism of the frames have been determined and investigated.

Retrofitted frame with cables passed through steel sheath shows appropriate behavior against cyclic loading with increasing amplitudes. The results show that these frames have a ductile behavior like steel moment frames and their energy dissipation capacity is the same as the main frame capacity. In this method, due to the lack of possibility of buckling, persistent deformation is not created in the frame and ductility required for the members is not increased by limiting relative displacement between classes by cables. In this retrofitting method, the axial force of the columns is limited and as a result, there less need to retrofit columns and foundations.

2. The Moment Frame Geometry and Retrofitted Frames

Behavior of moment frame without being retrofitted has been compared with the behavior of frames reinforced by double channel cross brace, cross cable brace, and brace with two cables passed through a cylindrical sheath at the junction of cables. These frames have been named as MF, MF-B, MF-C1 and MF-C2 respectively.

Members of the beam and columns of frames, profile H-150×150×7×10 is of SN400B mild steel. The design of the frames has been done with this philosophy that no collapse or buckling in the column should not be created in the event of a bounded frame failure. Also, in case of bounded failure, the behavior of the beam and column should be maintained. The used cable is of 316SUS type with a 7×19 strings and a nominal diameter of 10 mm, a Yield strength of 57.9 and a final strength of 2.60.2 kN. The braces have been made from 2UNP10 profile. Figure 1 shows the geometric characteristics of the moment and braced frames. The models details are listed in the Table 1.

Table 1. Model Details

Model	Beam profile	Column profile	Brace profile	Cable diameter (mm)
MF	H-150×150×7×10	H-150×150×7×10	-	-
MF-B	H-150×150×7×10	H-150×150×7×10	2UNP100	-
MF-C1	H-150×150×7×10	H-150×150×7×10	-	10
MF-C2	H-150×150×7×10	H-150×150×7×10	-	10

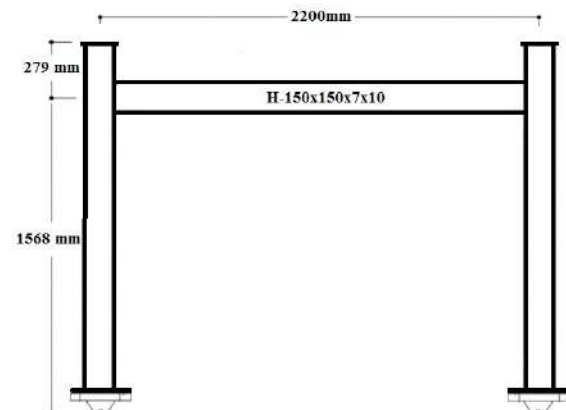


Figure 1. Geometric Characteristics of the Moment Frame

In a sample with cable brace and cylindrical steel sheath, specifications of the sheath include a length of 214, an internal diameter of 40 and a wall thickness of 15 mm. To prevent tension concentration and damage to the cable, the inside edge of the sheath has been rounded to a radius of 5 mm. Figure 2 indicates the finite element model of steel frame with cable brace. In these models, cyclic loading up to a maximum displacement of 300 mm has been used.



Figure 2. Finite Element Model of Moment Frame with Cable Brace

The deformation of the braced frame with the cable passed through the steel sheath is shown in Fig. 3 after exerting the lateral forces. In this frame, the cable length is greater than the diameter of the frame. Under the influence of the Q load, the frame begins to change. From the early stages of loading, tension occurs on all four cables when the member of the AB directly becomes straight ($\delta = \delta_s$). The cable shows a considerable resistance to the side movement. δ_s is determined due to the relative permitted displacement of the floor in the retrofitted frame and expected ductility from the moment frame. The relative displacement δ_s , in which the braces start to work, is calculated based on the length and diameter of the cylinder, the dimensions of the frame and allowable relative displacement between floors.

If the length of the cable inside the sheath is d_p , cable length out of sheath is L_B , the height of the frame and its length are h_c and h_b , δ_s is the lateral displacement created in the lateral frame deformation from the initial state to another state in which the frame diameter reaches the $2L_B + d_p$. By adjusting the L_B , the diameter and length of the sheath, the displacement can be limited by the permissible lateral change δ_s .

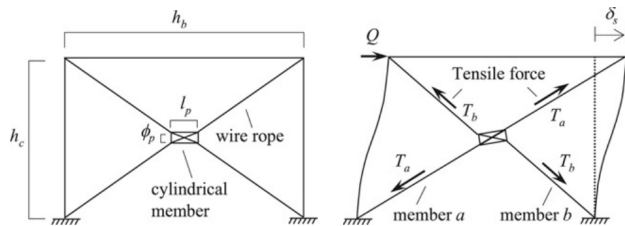


Figure 3. The Proposed System for the State with Cylindrical Member

3. Finite Element Model

The element used for the beam, column, and connector components is the reduced S4R hexagonal type with 4 knots and a linear order. Cable with a reduced element of type B31 has been modeled with two groups and a cross-section area equal to the effective cross-section of the cable.

In finite element model, nonlinear geometric behavior of materials and large deformations have been considered. For modeling of steel hardening

Isotropic and Kinematic compound has been implemented which shows a more accurate behavior in seismic loading^{[15][16][17][18][19][20][21][22]}.

Table 2 shows the specifications of consumed materials. Young's modulus of cylindrical sheath of steel has been introduced to be 1500 times the modulus of the mild steel in order to remove its deformation.

Table 2. Specifications of Consumed Materials

Steel	E (GPa)	F _y (MPa)	F _u (MPa)	Ultimate strain
SN400	180	2810	3310	0.2
SS400	180	2530	3330	0.19
A490	210	8020	9620	0.007

To prevent stress concentration at the location of cable contact with the sheath wall, the inner edge of the sheath is rounded to a radius of 5 mm. The collision in the beam-to-column connection has been modeled as a hard-frictional fitting with a detachment feature after unloading. For modeling the pre-stress force, 0.55 of tensile strength of the screw has been applied by using the thermal properties of materials with the local temperature reduction of the screw trunk^{[15][16][17][18][19]}.

At the cable connection point to the brace plate, the obtained concentration of tension and numerical instability hinder the progress of analysis. To avoid tension concentration, 12 rotational joint wire connectors were used for each cable at the cable connection to the latches^{[19][20][21][22]}. The loading of finite element models is considered as a cyclic lateral displacement with increasing amplitude. The appropriate size of the elements has been determined by analyzing the convergence of each member. The loading pattern is presented in Figure 4.

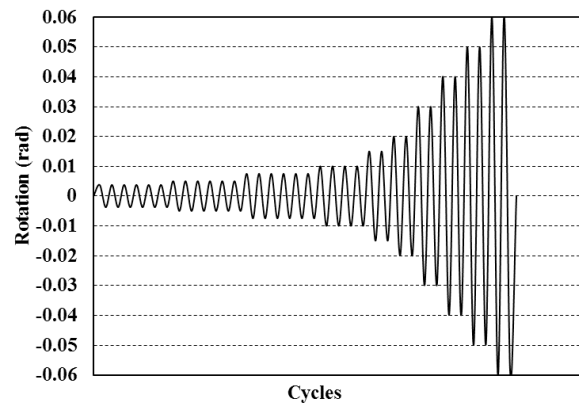


Figure 4. Loading Pattern

In Figure 5, curves resulted from the experimental and numerical work for the moment frame model of the steel with the sheath are shown. As it can be seen in the figure, loops of behavioral hysteresis curves in two finite element and laboratory modes are very close together in both methods and has a good compliance. As it can be seen in 50 mm lateral displacement, the descending stage of force-displacement curve is captured in the experimental model but there is no sign of reduction in finite element model. This is because of that experimental specimen failed in 55 mm lateral displacement and in the finite element model it is not considered.

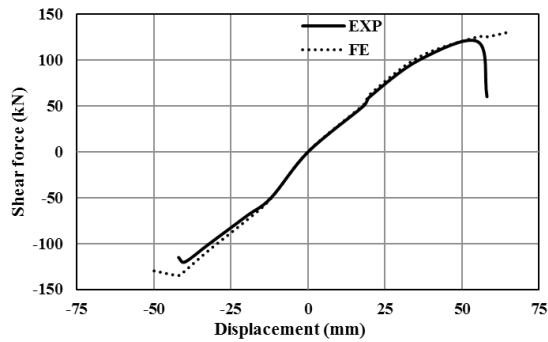


Figure 5a. Comparison of Experimental and Numerical Results – A Force-Displacement Graph

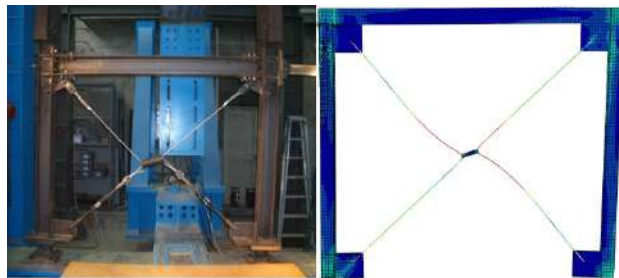


Figure 5b. Comparison of Experimental and Numerical Results – Deformation

4. Analysis of the Results

After analyzing the finite elements of these two models in Abaqus software, the obtained results will be observed in the visualization section. Therefore, the required results have been extracted and compared.

4.1 Plastic Strain and Stress Contour

In Figure 6, the contour related to the distribution of tension is shown in a variety of models. As it is seen in Figure 6a, in a conventional moment frame, tension concentration is situated at the location of column support and in the area of the beam connection to the column. The brace buckling occurs due to the compressive force in a moment frame with a conventional brace (Fig. 6b). As can be seen in Figure 6b, the stress concentration is situated in the location of column support and in the connecting area of the brace to the beam and column. Considering that buckling and large deformations occur in structural member of conventional brace during the first loading process and stiffness and resistance of the element is removed, it is impossible to use this member under pressure load. Due to the extreme tensile strength in a moment frame with a cable brace, one of the cables which is under the influence of tension and other one which is under pressure is left unused (Fig. 6c). Due to the presence of sheath in a moment frame with a sheathed cable brace, all frames and cables contribute to unloading

and it is expected that the cyclic behavior of the frame is symmetric (Fig. 6d).

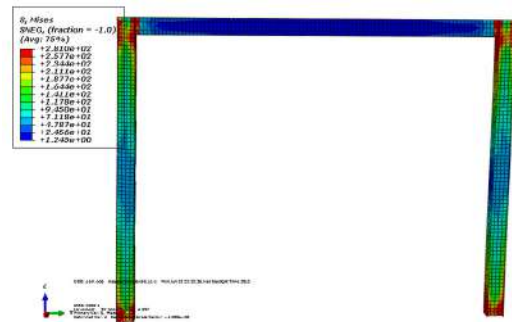


Figure 6a. Stress Contour of a Conventional Moment Frame

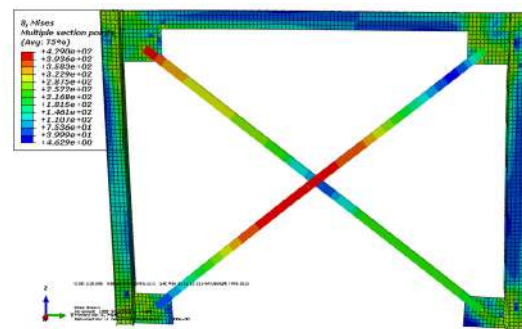


Figure 6b. Stress Contour of a Frame with Conventional Brace

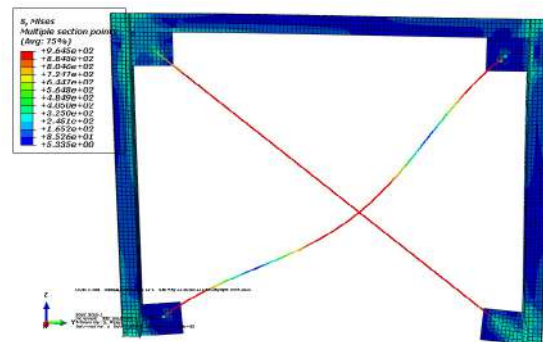


Figure 6c. Stress Contour of a Frame with Cable Brace

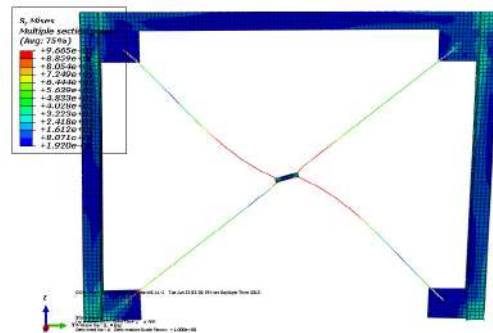


Figure 6d. Stress Contour of a Frame with Sheathed Cable Brace

In Figure 7, the contour related to the distribution of plasticity is shown in a variety of models. As it is shown in Figure 7a, the focus of plasticity in the conventional moment frame is situated is at the location of column support and in the area of beam-to-column connection. Due to the compressive force in the moment frame with conventional brace, buckling is made in the brace (Fig. 7b). As it can be seen in Figure 7b, focus of plasticity is on the location of column support and in the area of beam-to-column connection.

According to the extreme tensile strength in moment frame with cable brace, one of the cables which is under the influence of tension effect and other one which is under pressure is left unused and the major plasticity occurs at the linking point of cable to connecting plate of beam to the column (Fig. 7c). All the frames and cables have shares in each cycle of loading in a moment frame with a cable brace due to the sheath and plasticity occurs mainly in the sheath. Moreover, the rest of the structural components including the beam and the column are in the elastic state (Fig. 7d).

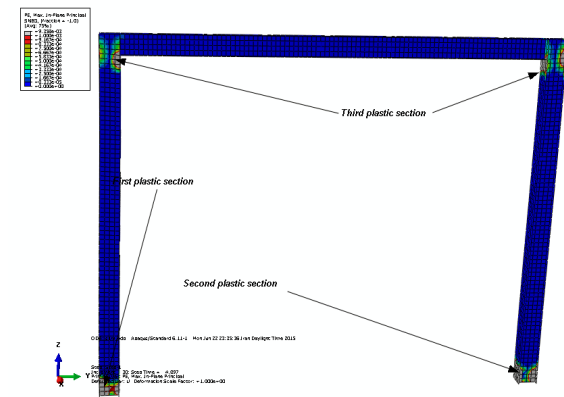


Figure 7a. Plasticity of a Conventional Moment Frame

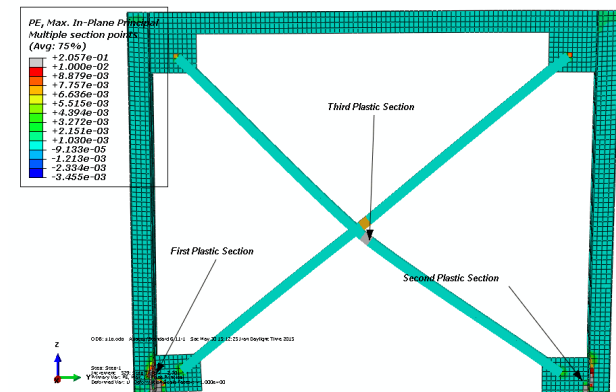


Figure 7b. Plasticity of a Frame with Conventional Brace

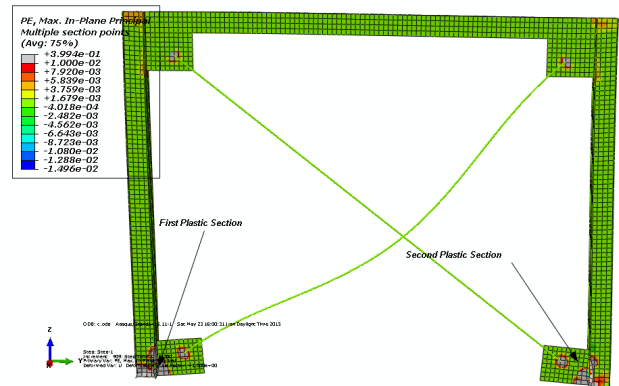


Figure 7c. Plasticity of a Frame with Cable Brace

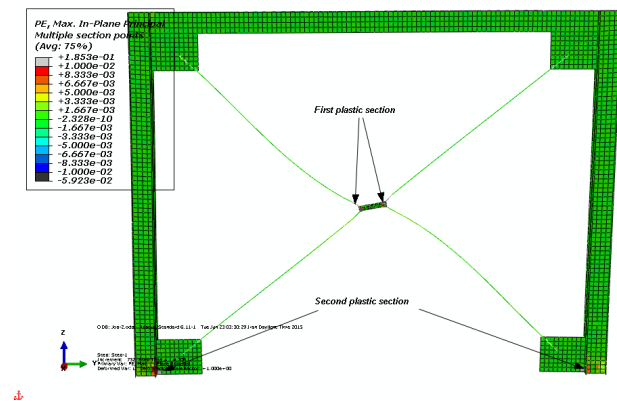


Figure 7d. Plasticity of a Frame with Sheathed Cable Brace

4.2 Hysteresis Graph

Figure 8a shows the force-displacement diagram in the moment frame under cyclic loading. As it can be observed, the hardness in the moment frame is very low. Stiffness is made due to the fact that lateral element loading is only the moment system of the frame. As it is shown in Figure 9a, this frame can withstand a maximum force of 211 kN.

According to Figure 8b, frame is associated with intangible losses after 30mm displacement in a moment frame with a cross brace based on Figure 8b, the mentioned frame can withstand 1250 kN in all cycles.

This means that the conventional brace shows uniform behavior in successive cycles, but the cycles have a small area. As it can be observed in Figure 8c, the frame faces a rupture in a moment frame with a conventional cable brace after 75 mm displacement. According to Figure 8c, this frame tolerates a maximum force of 1050 kN in the final cycle which means the cable brace has a high initial hardness, but its rupture occurs suddenly.

As it is seen in Figure 8d, after displacement of 30 mm in the moment frame with cross brace, the frame is accompanied by intangible losses. In Figure 8, the force-

displacement diagram of the moment frame with the sheathed cable brace under cyclic loading is demonstrated.

According to Figure 8d, this frame tolerates a maximum force of 1050 kN in all cycles. This means a conventional brace shows the uniform behavior successive cycles. Comparison of the graphs shown in Fig. 8 indicates that curve cycles in model of moment Frames with sheathed cable brace is more obese compared to other models.

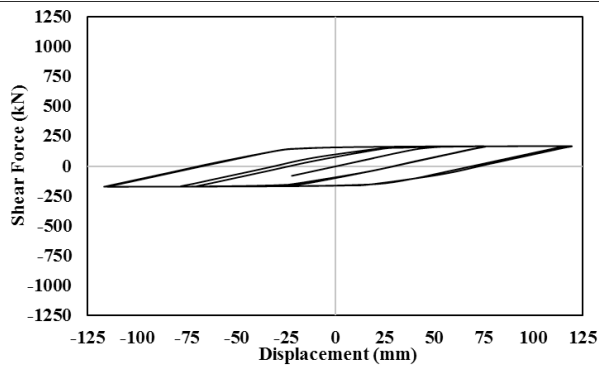


Figure 8a. Force-displacement Graph of a Conventional Moment Frame

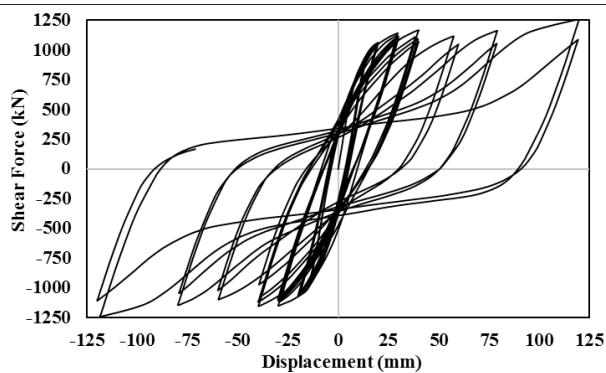


Figure 8b. Force-displacement Graph of a Frame with Conventional Brace

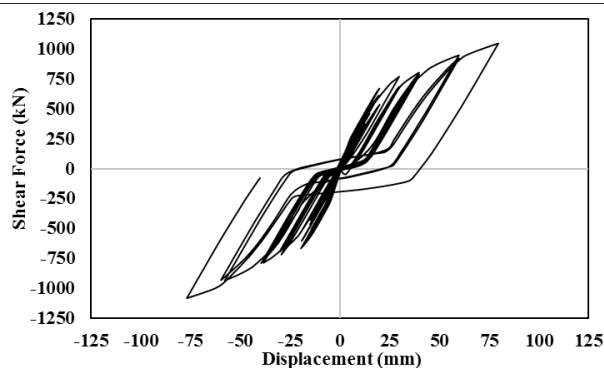


Figure 8c. Force-displacement Graph of a Frame with Cable Brace

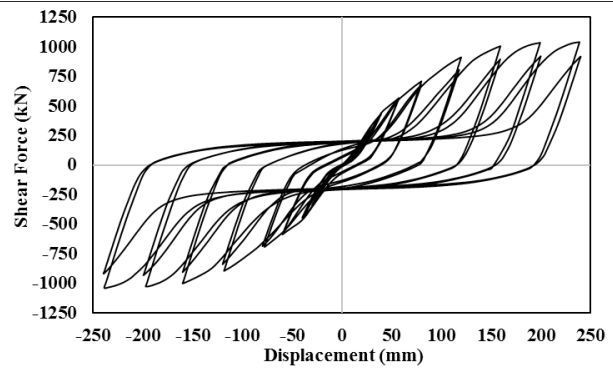


Figure 8d. Force-displacement Graph of a Frame with Sheathed Cable Brace

5. Dissipated Energy

Figure 9 shows the energy dissipated for a variety of models. As it can be seen, using sheathed cable brace increases the dissipation energy. The results of Figure 9 shows that braced frame and frame with sheathed cable brace dissipated energy more than other models.

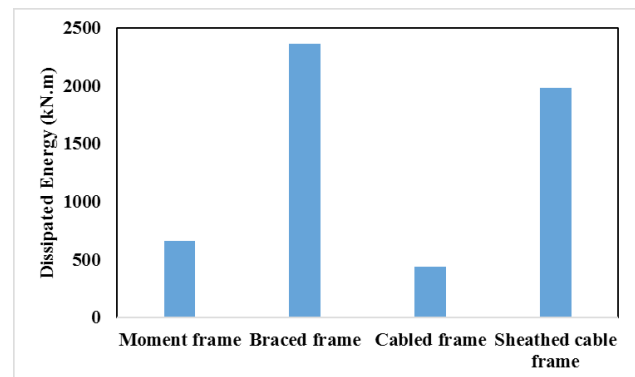


Figure 9. Dissipated Energy of Models

6. Conclusion

Finite element models of moment frame only and moment frame retrofitted with cable brace passed through a cylindrical steel sheath, cross brace with angles and cross brace with cable were created with the help of ABQUS software.

Nonlinear analysis of frames under cyclic loading has been done with increasing ranges. Comparison of numerical analysis results and experimental outcomes shows the accuracy of finite element models.

Basic cut, plasticity, cyclic force-displacement behavior and exact tension concentration have been precisely determined and reviewed.

The use of double channels for reinforcing steel moment frame leads to significant increase in the initial hardness and final load of the frame and results in decline in the final displacement. Reduced ductility and

energy dissipation capacity indicates that the permanent deformation is created in the frame due to the buckling of the compressive member in this type of retrofitting. In the frame reinforced with cross brace, the cables work from the early stages of loading to the tension and increase the initial stiffness of the frame in comparison with the hardness of the moment frame. In this case, the final load increases and the failure displacement decreases. In the mentioned frame, the cable brace transforms the frame's behavior from a ductile behavior to brittle behavior. Moreover, the results show that using sheathed cable brace increases the dissipation energy.

Narrow and unstable hysteresis cycles demonstrate the small capacity of this frame to resist lateral forces. In this method of reinforcement, retrofitting of columns and foundation is remarkable. The initial stiffness of the frame is the same for both the sheathed-cable brace and the moment frame. Force displacement diagrams of the two mentioned frames are consistent until the displacement of the δ_s . The cable does not affect the moment frame behavior up to the noted amount of displacement and straightening brace. Then, in the event of an invasion of forces from lateral forces such as δ_s , brace contribute to the frame's behavior with delay. Consequently, the behavior of the frame is a form of ductile behavior of moment frame up to displacement of δ_s . By adding brace to these frames, resistance of the frame is increased while its ductility is maintained. In this retrofitting method, due to the lack of possibility of buckling, persistent deformation cannot be made. In addition, required ductility for the members is not increased by limiting relative displacement between floors using cables.

References

- [1] Rahnavard, R., Hassanipour, A., Suleiman, M., Mokhtari, A. (2017). Evaluation on eccentrically braced frame with single and double shear panel. *Journal of Building Engineering*, 10, 13–25
- [2] Rahnavard, R., Fard, F. F. Z., Hosseini, A., Suleiman, M. (2018). Nonlinear analysis on progressive collapse of tall steel composite buildings. *Case Studies in Construction Materials*. 8. 359–379
- [3] Rahnavard, R., Siahpolo, N., Function comparison between moment frame and moment frame with centrally braces in high-rise steel structure under the effect of progressive collapse. *Journal of Structural and Construction Engineering*.4(4). Serial Number 14, 42-57. DOI: 10.22065/jsce.2017.77865.1084
- [4] Tamai, H. and Takamatsu, T. Cyclic loading tests on a non-compression brace considering performance based seismic design, *Journal of Constructional Steel Research*, 61(9), 1301-1317 (September 2005).
- [5] Bartera, F. and Giacchetti, R., (2004). Steel dissipating braces for upgrading existing building frames, *Journal of Constructional Steel Research*, 60(3), 751-769
- [6] Rahnavard, R., Hassanipour, A., (2015). Steel Structures analysis using ABAQUS, *Kerman: Academic Center for Education, Culture and Research*, Publishing Organization of Kerman branch
- [7] Rahnavard, R., Hassanipour, A., Mounesi, A., (2016). Numerical study on important parameters of composite steel-concrete shear walls. *Journal of Constructional Steel Research*. 121 441–456
- [8] Rahnavard, R., Naghavi, M., Abudi, M., Suleiman, M., (2018). Investigating Modeling Approaches of Buckling-Restrained Braces under Cyclic Loads, *Case Studies in Construction Materials*. 8. 476–488
- [9] Naghavi, M., Rahnavard, R., Thomas, R. J., Malekinejad, M., (2019). Numerical evaluation of the hysteretic behavior of concentrically braced frames and buckling restrained brace frame systems. *Journal of Building Engineering*. 22. Pages 415-428
- [10] Naghavi, M., Malekinejad, M., (2018). A Study of the Behavior of Steel Moment Frame with Buckling Restrained Bracing (Review Article). *Soil Structure Interaction Journal*. 3(1)
- [11] Xie, Q. (2005). State of the art of buckling-restrained braces in Asia. *Journal of Constructional Steel Research*. 61(6), 727-748
- [12] Sun, H., Jia, M., Zhang, S., Wang, Y., (2019). Study of buckling-restrained braces with concrete infilled GFRP tubes. *Thin Walled Structures*, 136, 16-33
- [13] Hou, X., Tagawa, H. (2009). Displacement-restraint bracing for seismic retrofit of steel moment frames. *Journal of Constructional Steel Research*, 65 1096–1104
- [14] ABAQUS, Inc., Ver. 6.9, Analysis User's Manual (2010)
- [15] Rahnavard, R., Thomas, R. J., (2018). Numerical Evaluation of the Effects of Fire on Steel Connections; Part 1: Simulation Techniques. *Case Studies in Thermal Engineering*. Vol 12, page 445-453
- [16] Rahnavard, R., Thomas, R. J., (2019). Numerical Evaluation of the Effects of Fire on Steel Connections; Part 2: Model results. *Case Studies in Thermal Engineering*, 13. DOI: <https://doi.org/10.1016/j.csite.2018.11.012>
- [17] Rahnavard, R., Siahpolo, N., Naghavi, M., Hassanipour, A., (2014). Analytical Study of Common Rigid Steel Connections under the Effect of Heat. *Advances in Civil Engineering*. 2014, Article

- ID 692323. DOI:10.1155/2014/692323
- [18] Hassanipour, A., Rahnavard, R., Mokhtari, A., Rahnavard, N., (2016). Numerical investigation on reduces web beam section moment connections under the effects on cyclic loading. *J. Multidiscip. Eng. Sci. Technol. (JMEST)*, 2(8), 3159-0040
- [19] Rahnavard, R., Khaje, M. T., Hassanipour, A., Siahpolo, N., (2017). Parametric Study of Seismic Performance of Steel Bridges Pier Rehabilitated with Composite Connection. *Journal of Structural and Construction Engineering*. DOI: 10.22065/JSC.2017.92128.1259
- [20] Rahnavard, R., Hassanipour, A., Siahpolo, N., (2015). Analytical study on new types of reduced beam section moment connections affecting cyclic behavior. *Case Studies in Structural Engineering*, 3, 33-51
- [21] Radkia, S., Gandomkar, F. A., Rahnavard, R., (2018). Seismic Response of Asymmetric Sliding Steel Structure with Considering Soil-Structure Interaction Effects. *Journal of Structural and Construction Engineering*. DOI: 10.22065/JSC.2018.105638.1384
- [22] Radkia, S., Rahnavard, R., Gandomkar, F. A., (2018). Evaluation of the effect of different seismic isolators on the behavior of asymmetric steel sliding structures. *Journal of Structural and Construction Engineering*. DOI: 10.22065/JSC.2018.114089.1428

ARTICLE

Numerical Study of the Behavior of Steel Frame with Concentric Buckling Restrained and Conventional Braces

Mohammad Naghavi^{1*} Mohsen Malekinejad²

1. Department of Civil Engineering, Javid Institute for Higher Education of Jiroft, Iran

2. Department of Civil Engineering, Islamic Azad University, Sirjan Branch, Iran

ARTICLE INFO

Article history

Received: 1 April 2019

Accepted: 26 August 2019

Published: 31 August 2019

Keywords:

Buckling restrained braces

Concentric conventional braces

Plasticisation

Static nonlinear analysis

ABSTRACT

In this paper, a method is proposed to provide a simple model of buckling restrained braces. After introducing the elements, taking into account all parts of buckling restrained braces, a sample of this type of braces is modeled in finite element Abaqus software. After confirming the numerical model using the available laboratory results, which is carried out by static nonlinear analysis, moment frame model with chevron bracing is compared with moment frame with chevron buckling-restrained bracing. In this study, the behavior of buckling restrained braces as a hysteretic damper was investigated and a good performance was observed in energy absorption compared to conventional bracing.

1. Introduction

Several types of control systems including active, semi-active and passive control systems have been developed to systematically control the structure under destructive effects of earthquakes^{[1][2][3][4][5]}. The Buckling-Restrained Bracing Frame (BRBF) is a new type of braced system with energy dissipation that uses to improve the behavior of concentric brace frames. In this system, the brace element is placed in a sheath that prevents buckling of the element. With this equipment, the behavior of the brace is the same as its behavior in tension with yielding (rather than buckling) under pressure, and thus resulting in improved ductility and energy dissipation than in conventional braces. The elastic stiffness of the bracing frames is comparable in terms of the stiffness of

the frames that have eccentric braces. The results of real-dimensional experiments on these members show that the equipped frames with buckling restrained systems using this method and proper implementation details are included. These systems show stable and symmetrical behavior under pressure and elasticity, and even in very large deformations^{[1][2][3][4][5]}. In addition, the ductility and energy-absorbing capacity of these frames are in the range of special steel moment frames (steel frames with a high ductility) and more than special bracing frames, which is a result of the high level of ductility resulting from the enclosure of the steel core of the braces against buckling^{[1][2][3]}. In order to prevent possible damage to existing buildings in future earthquakes and to develop these buildings, their performance and their behavior are

*Corresponding Author:

Mohammad Naghavi,

Department of Civil Engineering, Javid Institute for Higher Education of Jiroft, Iran

Email: mn147013@gmail.com

quintessential. Methods of reinforcing these structures as well as their design criteria are possible in different ways. The reinforcement of steel frames by using bracing systems has been considered by many researchers as one of the most practical and effective methods^{[4][5][6][7][8][9][10]}. Therefore, it is necessary to develop the use of steel braces conducting a number of investigations. The results of experiments carried out in 2002 on buckling restrained braces showed that the gusset plates actually created a rigid opening and the rotation of the nodes would be considered due to the high rigidity of the gusset plate in analysis and design^[7]. Rahnavard et al. (2018) studied the numerical methods of buckling restrained bracing modeling. They presented the method of using spring as an alternative method for modeling concrete and casing, the results of which were more accurate than the complete modeling of concrete and casing^{[8][9][10][11][12]}. In 2005, Choi and Kim, using the hysteretic energy spectrum, presented a method for designing frames equipped with buckling restrained braces^[13]. In this method, it is assumed that the beams and columns remain under gravity loads in an elastic state, and energy dissipation and the resulting damage occur only in buckling restrained braces. In 2006, Fahnestock and his colleagues presented a research program on buckling restrained braces^[14]. Jea et al. (2014) studied and compared the analysis of the periodic function of moment frame system with buckling restrained brace and moment frame without bracing. Their results showed that moment frame with buckling restrained braces tolerated shear force more than twice that of a moment frame without bracing^[15].

1.1 Buckling Restrained Braces

Shocking statistics published on the status of existing buildings, the observation of urban construction and a look at the causalities and financial losses of earthquakes in recent years, is an indicative of the vulnerability of most of the existing buildings in the face of a relatively severe earthquake. With this in mind, precise control over the calculation and execution of buildings is an important factor in preventing or reducing casualties is necessary. However, it should be noted that there are a bulk of buildings built in the past, and some actions should be taken to improve their seismic performance. In addition, buildings damaged by earthquakes need structural reinforcement, due to several factors including the following:

- Due to their lack of sufficient lateral stiffness and strength, these structures require lateral reinforcement and drift control.
- Due to some weaknesses, such as infilled frames or brick infilled frames as part of a seismic isolation system,

or the inability to use suitable bracing or ductility systems, there is a potential for sudden and crisp destruction, and as a result, in addition to damages to the structure, there is no chance for escape from the collapse of the inhabitants, and casualties will increase.

- It may be necessary to increase the number of floors, increase the level of floors, or change in utilization. Due to the increase in loads and the change in the structural characteristics of the structure, reinforcement may be needed

The idea of using a yielding steel element to absorb energy was introduced more than 30 years ago. The new approach was to squeeze the compression element before buckling. The important point is that the yielding does not take place locally and its distribution throughout the element is appropriate and uniform, so that the depreciated energy reaches its maximum during a reciprocal loading, such as an earthquake. This research was based on the prevention of buckling of the compression bracing using concrete coating around it. In this kind of braces, the pressure bearing is obstructed by the steel core, and the concrete coating only prevents the buckling of the steel core, which causes the lateral distribution of the internal pressure in the coating concrete^{[3][4][5][6]}. Figure 1 shows the ideal behavior of the buckling-restrained brace.

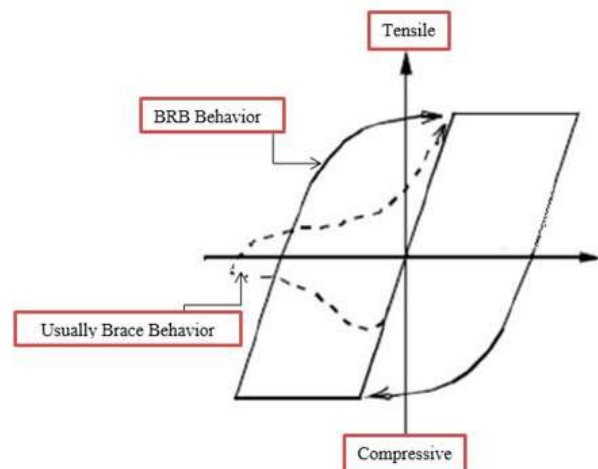


Figure 1. The Ideal Behavior of Buckling-restrained Brace^[9]

In order to avoid the axial compressive force transmitted to the concrete from the steel core, a thin layer of special material is placed on the joint surface of steel and concrete. This layer, by preventing the friction between the core and the concrete, transmits the compressive force due to the lateral displacement of the core steel to a single wide load transverse to concrete. Ultimately, this way of transferring force in the buckling element has led to the use of this type of braces as an

unbonded brace. Figure 2 shows a variety of buckling restrained braces.

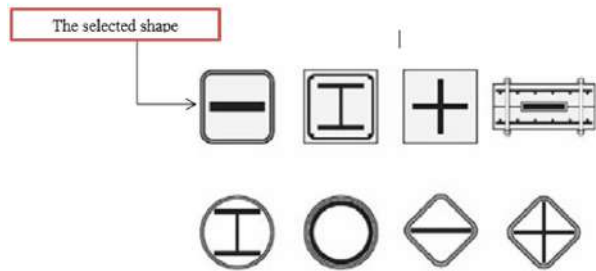


Figure 2. Variants of Buckling Restrained Braces

The use of this type of braces began in Japan in the 1980s. In the 1990s, researchers from the United States carried out extensive research on unbounded braces, which led to the use of this type of braces in various buildings to improve seismic rehabilitation. The research is ongoing in other countries in the world, including India and Taiwan. The devastating consequences of an earthquake, combined with loss of life and economic damage, make it more important than ever to perceive the proper understanding of the behavior of structures under earthquake vibratory stimulations. This is one of the main concerns of civil engineers in designing various structures and forcing them to design strong structures against earthquake forces. In the design of structures, a combination of resistance, ductility and energy absorption capacity should be provided. Given that the inherent capacity of most structures to absorb energy from earthquake forces is very low, a certain level of ductility and vulnerability in structures will be acceptable. The damages to structures are largely unrecoverable and will result in high economic costs. The use of buckling braces can significantly increase the energy absorption capacity of the structure and ultimately reduce structural damage^{[3][4][5][6]}.

In this research, moment frame modeling with chovern conventional brace and moment frame with chovern buckling restrained brace are compared with each other using finite element method and using ABAQUS. Moreover, new method for BRB modeling is presented.

2. Numerical Modeling

The purpose of such studies is to estimate and calculate the design parameters of these elements. In this step, loading will only be done in the form of reciprocal displacement. The loading procedure in this case is considered as a linear increase load applied to the two ends of the columns as a cyclic loading. Given that in the step stage, the analytical method is nonlinear static, so it

is possible to study the nonlinear behavior of the models. In Figure 1, the overall model used for conventional and buckling restrained braces is shown. These models are called VCBF (Shervon CBF) and VBRB (Shervon BRB), respectively. The length of the openings in this model is 6 meters and the height of each floor is 3.4 meters. The sections IPE27 and 2IPE27 are considered respectively for columns and beams. Also, 2UNP12 and PL110 × 10 mm were used for conventional and buckling restrained braces.

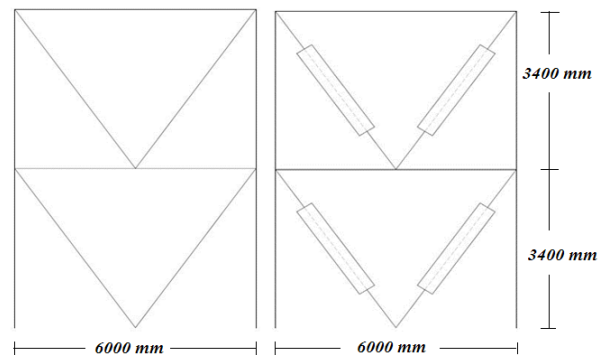


Figure 3a. Moment Frame Model with Conventional Chovern Brace (VCBF)

Figure 3b. Moment Frame Model with Buckling Restrained Chovern Brace (VBRB)

In this section, for evaluating and comparing the laboratory sample and numerical model, we study the modeling of the moment frame with buckling restrained braces. To achieve this goal, the laboratory model of Jea et al. was selected^[15]. Figure 4 shows the geometric dimensions of the laboratory model. A spring was used for modeling the casing and filler concrete. All parts of the model were also performed using the S4R shell element. This element has four nodes and six degrees of freedom for each node. To determine the mechanical properties of steel, the value of the elasticity module is 210 GPa, and the amount of final yielding and stress for the core are 263 MPa and 379 MPa, for beams 261 MPa and 413 MPa, and for the enclosing steel and the column are 298 MPa and 366 MPa, respectively. Steel hardness is also used for isotropic and kinematic combinations. This hardening shows a good behavior in cyclic loading^{[16][17][18][19][20][21][22][23][24][25][26]}. To load the models of this research, two types of near and far loading SAC have been used (Figure 4). Figure 5 shows a kernel-spring numerical model. In Fig. 6, we show curves drawn from laboratory and numerical models or springs. As can be seen in the figure, the behavioral hysteresis curves in both the software and the laboratory are very close in each case and have a good fit.

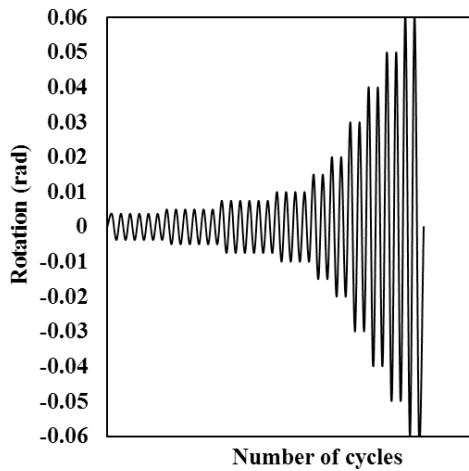


Figure 4a. Sac Cyclic Loading (Far Fault)

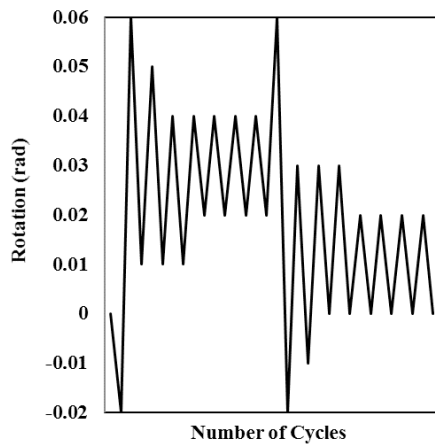


Figure 4a. Sac Cyclic Loading (Near Fault)

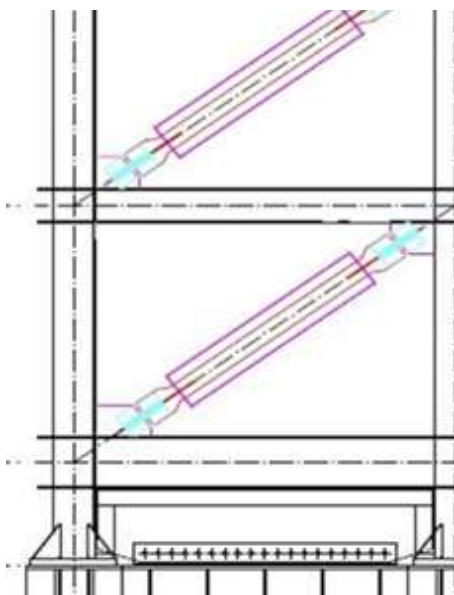


Figure 5. Geometry of the Laboratory Model (mm) ^[14]

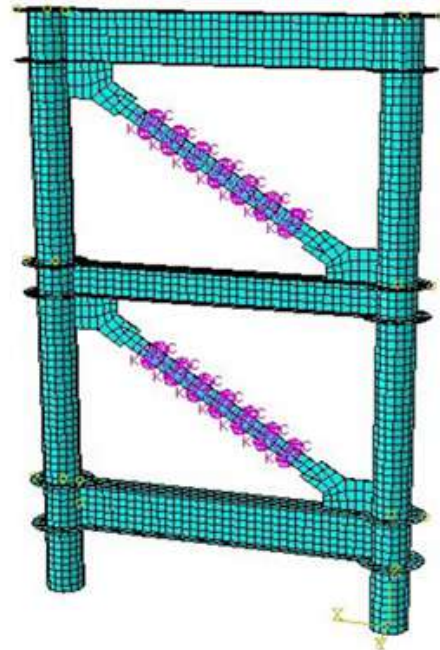


Figure 6. Numerical Model Constructed Based on Laboratory Model [14]

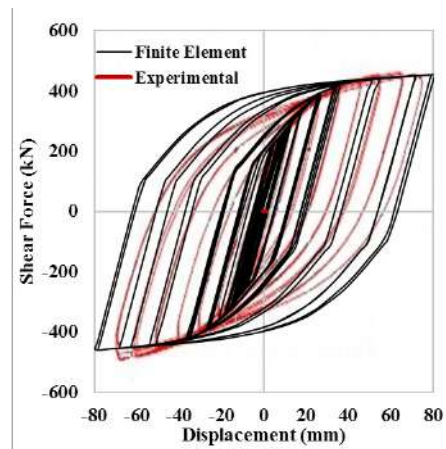


Figure 7. Comparison of Hysteresis Curves of the Numerical Model and Laboratory Samples

3. Analysis of Results

After finite element analysis of these two models in the Abaqus software, the results will be visible in the Visualization section. Therefore, the required results have been extracted and compared.

3.1 Plastic Stress and Strain Contour

In Fig. 8, the contour related to the distribution of stress in a moment frame with a conventional brace and a moment frame with buckling restrained braces is shown. As can be seen, in the conventional brace, the focus of stress in the middle of the opening has led to the buckling of the brace and the intermediate beam. In

the buckling restrained brace, there is no buckling due to the bracing of the steel core. On the other hand, by observing the distribution of stress in the steel core, as shown in Fig. 8b, due to the stress distribution along the steel element, the maximum stress in this element has also been reduced. Given that in the conventional brace, the structural element experiences buckling and enlarged deformation during the first loading process, and that the hardness and strength of the element disappears, so it makes it impossible to use this member under pressure load. Consequently, in buckling restrained braces, due to improved compression strength of the member, these types of braces can be used to withstand tensile and compressive loads.

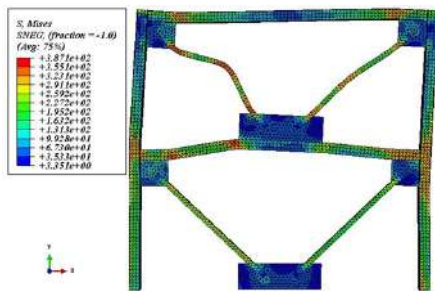


Figure 8a. Conventional Brace Stress Contour

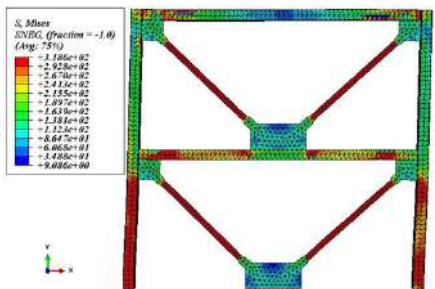


Figure 8b. Buckling Restrained Brace Stress Contour

In Fig. 9, the plastic strain distribution contour related to moment frame with a conventional brace and moment frame with buckling restrained braces is shown. As can be seen, in conventional brace, the focus of plasticization is in the middle of the opening, the brace and the gusset spring of the column. On the other hand, by observing the distribution of plastic strain in the steel core, as shown in Fig. 9b, due to the strain distribution along the steel member, its intensity in other elements was reduced. Due to the fact that in the conventional brace, the structural member during the first loading process is plasticised and the stiffness and strength of the element disappears, it is impossible to use this member under pressure load. Consequently, in buckling restrained braces, due to improved compression resistance of the member, these types of braces can be used to dissipate energy in the

plastic region. To explain the same distribution observed along the conventional brace for both the stress and the strain, it is probably due to the proportionality between the stress and the strain.

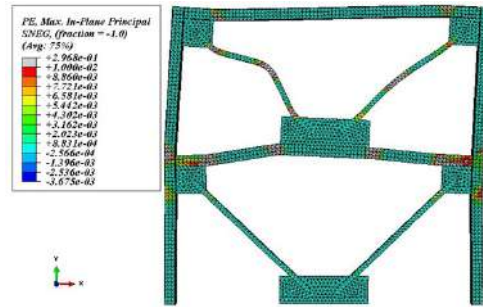


Figure 9a. Stress Contour of Conventional Brace

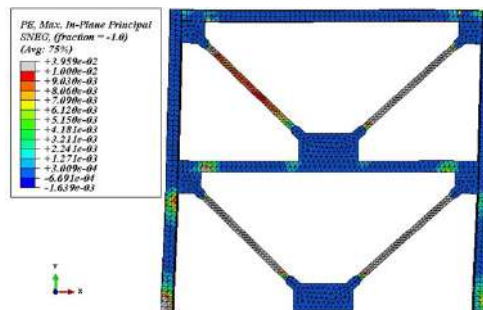


Figure 9b. Buckling Restrained Brace Stress Contour

3.2 Evaluation of Hysteresis Curve Under Far Load Pattern

In Fig. 10, the force-displacement diagram of the moment frame with a conventional brace and the moment frame with buckling restrained braces is shown under a far loading pattern. As it is seen, in the moment frame with a conventional brace, after a 30 mm displacement, the frame is accompanied by a sharp collapse. The reason for this deterioration is the buckling resistance of the brace under the influence of compressive force. As shown in Fig. 10a, this frame tolerates the force of 1800 kN in the first cycles, but after the bracing buckling, the shear force is about 950 kN. As seen in Fig. 10b, in the moment frame with buckling restrained brace, after a 300mm displacement, the frame experiences with an intangible collapse. As shown in Fig. 10b, this frame can withstand 1800 kN in all cycles. This means that the buckling restrained brace shows a uniformity of behavior in successive cycles. Comparison of the two diagrams shown in Figure 10 shows that the resistance decline in the moment frame with buckling restrained brace (300 mm) decreases by up to 10 times compared to the moment frame with the buckling brace (30 mm). Moreover, the curving cycles in the moment frame model with the buckling restrained braces are more obtuse.

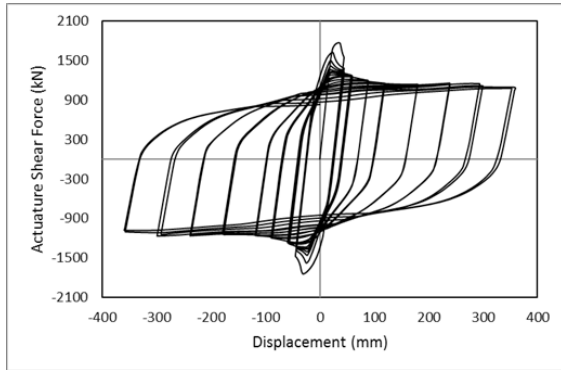


Figure 10a. Force-displacement Diagram under the Influence of Far Pattern (Frame with Conventional Brace)

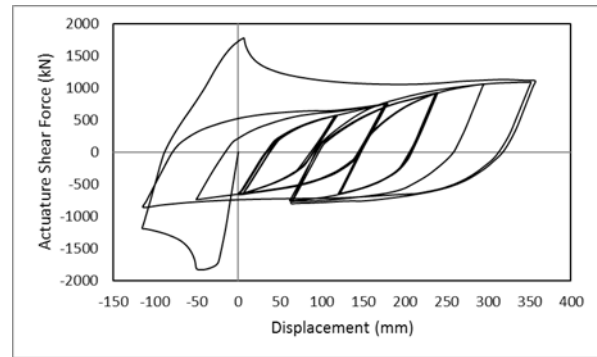


Figure 11a. Force-displacement Diagram under the Influence of Near Pattern (Frame with Conventional Brace)

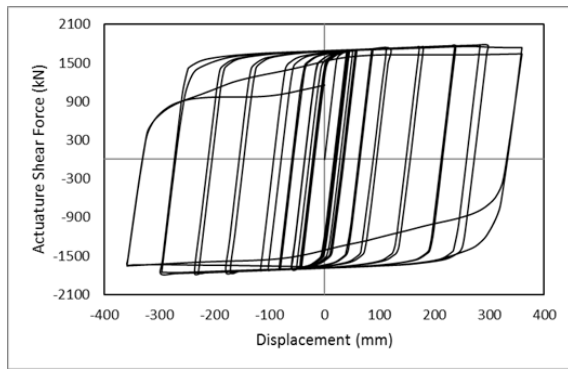


Figure 10b. Force-displacement Diagram under the Influence of Far Pattern (Frame With Buckling Restrained Brace)

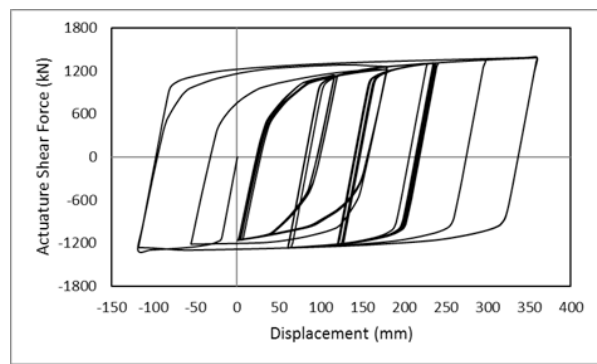


Figure 11b. Force-displacement Diagram under the Influence of Near Pattern (Frame with Buckling Restrained Frame)

3.3 Evaluation of Hysteresis Diagram under Near Load Pattern

In Fig. 11, the force-displacement diagram in the moment frame with a conventional brace and a moment frame with buckling restrained braces is shown under near loading pattern. As it is seen, in the moment frame with a conventional brace, after 50 mm displacement, the frame is associated with a severe collapse. The reason for this deterioration is the buckling resistance of the brace under the influence of compressive force. As shown in Fig. 11a, this frame can withstand a force of 1,750 kN in the first cycles, but after buckling, the shear force is about 850 kN. As seen in Fig. 11b, in the moment frame with buckling brace, after displacing a 350mm the frame experiences an intangible collapse. As shown in Fig. 11b, this frame can withstand 1800 kN in all cycles. This means that the buckling brace shows a uniformity of behavior in successive cycles. The comparison of the two diagrams in Fig. 11 shows that resistance reduction in the moment frame with the buckling restrained brace is up to 7 times as compared to the moment frame with the buckling brace. Also, the curving cycles in the moment frame model with the buckling restrained braces are much more obtuse.

4. Conclusion

In this study, using finite element method, two moment frame models with conventional chovern brace and with buckling chovern brace were compared under SAC far and near loading patterns. The use of buckling restrained braces led to increased bracing strength and ductility. Therefore, it creates a symmetry in the resistance of the element under the axial load of the strain and compression, and therefore the full capacity of braces in strain and pressure is used in the structural frame systems in which the braces are used double. Given that the main task of braces is to withstand lateral loads, the use of buckling restrained braces, in addition to increasing the safety of the structure, will make the rest of the structure thin, making the design more economical. The use of buckling restrained braces makes the structure of the frame function symmetrical, and therefore the performance of these structures will be improved against actual loads such as earthquakes that have reciprocal nature. Proper reinforcement, based on ease in executive problems as well as economic considerations, provides this structural optimization method with a very good performance for resistance, stiffness and ductility, which is one of the

basic principles for an optimization plan. Also, the results indicate that collapse in resistance in buckling bracing system is 10 times slower than the conventional frame system. Moreover, this results are supported by other research investigation^[10].

References

- [1] American Institute of Steel Construction, Inc. (AISC). (1999). Load and Resistance Factor Design Specification for Structural Steel Buildings. AISC, Chicago, IL, December 27.
- [2] Rohola Rahnavard, Robert J. Thomas, (2019). Numerical evaluation of steel-rubber isolator with single and multiple rubber cores, *Journal of Engineering Structures*, <https://doi.org/10.1016/j.engstruct.2019.109532>
- [3] El-Tayem, A. A., and Goel, S. C. (1986). Effective Length Factor for the Design of X-bracing Systems. *Engineering Journal*, AISC, vol. 24, page 41-45.
- [4] El-Tayem, A. A., and Goel, S. C. (1986). Cyclic Load Behavior of Angle X-Bracing. *Journal of Structural Engineering*, vol. 112, Issue 11, pages 2528-2539.
- [5] Kathib I. F., Mahin, S. A. (1987). Dynamic inelastic behavior of chevron braced steel frames. Fifth Canadian Conference on Earthquake Engineering, Balkema, Rotterdam, pages 211-220. Perotti, F., and Scarlassara, P. (1991). Concentrically Braced Steel Frames under Seismic Actions: Non-linear Behavior and Design Coefficients. *Earthquake Engineering and Structural Dynamics*, vol. 20, pages 409-427.
- [6] Elghazouli, A. Y. (2003). Seismic design procedures for concentrically braced frames. *Proceedings of the Institution of Civil Engineers: Structures and Buildings*. volume 156, issue 4. Pages 381-394.
- [7] Lopez, W. A., Gwie, D. S., Saunders, C. M., Lauck, T.W., (2002), "Lessons learned from largescale tests of unbonded braced frame subassemblages", *Proceedings 71st Annual Convention*, Structural Engineers Association of California, Sacramento, California.
- [8] Rohola Rahnavard, Akbar Hassanipour, (2015). Steel Structures analysis using ABAQUS, Kerman: Academic Center for Education, Culture and Research, Publishing Organization of Kerman branch
- [9] Rohola Rahnavard, Mohammad Naghavi, Maryam Abudi, Mohamed Suleiman, (2018). Investigating Modeling Approaches of Buckling-Restrained Braces under Cyclic Loads, *Case Studies in Construction Materials*, *Case Studies in Construction Materials* 8 476-488
- [10] Mohammad Naghavi, Rohola Rahnavard, Robert J. Thomas, Mohsen Malekinejad, (2018). Numerical evaluation of the hysteretic behavior of concentrically braced frames and buckling restrained brace frame systems, *Journal of Building Engineering*, Volume 22, Pages 415-428
- [11] Rohola Rahnavard, Akbar Hassanipour, Ali Mounesi, (2016). Numerical study on important parameters of composite steel-concrete shear walls, *Journal of Constructional Steel Research* 121 441-456.
- [12] Rohola Rahnavard, Akbar Hassanipour, Mohamed Suleiman, Ali Mokhtari, (2017). Evaluation on eccentrically braced frame with single and double shear panel, *Journal of Building Engineering* 10 13-25
- [13] Choi, H., Kim, J., (2006), "Energy-based seismic design of buckling-restrained braced frames using hysteretic energy spectrum", *Engineering Structures*, 28(2006), 304-311.
- [14] Fahnestock, L. A., Sause, R., and Ricles, J. M., (2006), "Seismic response and performance of buckling-restrained braced frames", *Journal of Structural Engineering*, ASCE, September 2007, pp. 1195-1204.
- [15] Mingming Jia, Dagang Lu, Lanhui Guo, Lin Sun, Experimental research and cyclic behavior of buckling-restrained braced composite frame, *Journal of Constructional Steel Research* 95 (2014) 90-105.
- [16] Rohola Rahnavard, Robert J. Thomas, (2018). Numerical Evaluation of the Effects of Fire on Steel Connections; Part 1: Simulation Techniques, *Case Studies in Thermal Engineering*. Vol 12, page 445-453
- [17] Rohola Rahnavard, Robert J. Thomas, (2018). Numerical Evaluation of the Effects of Fire on Steel Connections; Part 2: Model results, *Case Studies in Thermal Engineering*. Vol 13, <https://doi.org/10.1016/j.csite.2018.11.012>
- [18] Sahar Radkia, Rohola Rahnavard, Farhad Abbas Gandomkar, (2018). Evaluation of the effect of different seismic isolators on the behavior of asymmetric steel sliding structures, *Journal of Structural and Construction Engineering*, doi: 10.22065/JSCE.2018.114089.1428
- [19] R Rahnavard, A Hassanipour, N Siahpolo, (2015). Analytical study on new types of reduced beam section moment connections affecting cyclic behavior, *Case Studies in Structural Engineering* 3, 33-51.
- [20] Kelly, J. M., Skinner, R. I., and Heine, A. J., (1972), "Mechanism of energy absorption in special devices for use in earthquake resistant structures", *Bull. N.Z. Nat. Soc. Earthquake Eng.* 5(3):63-88.
- [21] Rohola Rahnavard, Navid Siahpolo, Mohammad

- Naghavi, Akbar Hassanipour, (2014). Analytical Study of Common Rigid Steel Connections under the Effect of Heat, *Advances in Civil Engineering*, vol. 2014, Article ID 692323, 10 pages. doi:10.1155/2014/692323
- [22] Akbar Hassanipour, Rohola Rahnavard, Ali Mokhtari, Najaf Rahnavard, (2016). Numerical investigation on reduces web beam section moment connections under the effects on cyclic loading”, *J. Multidiscip. Eng. Sci. Technol.(JMEST)* 2 (8), 3159-0040
- [23] Rohola Rahnavard, Mazyar Taghi Khaje, Akbar Hassanipour, Navid Siahpolo, (2017). Parametric Study of Seismic Performance of Steel Bridges Pier Rehabilitated with Composite Connection”, *Journal of Structural and Construction Engineering*, (DOI): 10.22065/JSCE.2017.92128.1259
- [24] Rohola Rahnavard, Faramarz Fathi Zadeh Fard, Ali Hosseini, Mohamed Suleiman, (2018). Nonlinear analysis on progressive collapse of tall steel composite buildings, *Case Studies in Construction Materials* 8 359–379
- [25] Sahar Radkia, Farhad Abbas Gandomkar, Rohola Rahnavard, (2018). Seismic Response of Asymmetric Sliding Steel Structure with Considering Soil-Structure Interaction Effects, *Journal of Structural and Construction Engineering*, doi: 10.22065/JSCE.2018.105638.1384
- [26] Rohola Rahnavard, Navid Siahpolo, (2017). “Function comparison between moment frame and moment frame with centrally braces in high-rise steel structure under the effect of progressive collapse, *Journal of Structural and Construction Engineering*, Volume 4, Issue 4 - Serial Number 14, Page 42-57, doi: 10.22065/jsce.2017.77865.1084

ARTICLE

Feasibility Study on Use of Plastic Waste as Fine Aggregate in Concrete Mixes

Sudarshan D. Kore

School of Construction Management, National Institute of Construction Management and Research (NICMAR), Balewadi, Pune, India

ARTICLE INFO

Article history

Received: 1 April 2019

Accepted: 26 August 2019

Published: 20 November 2019

Keywords:

Plastic waste

Concrete

Mechanical Properties

ABSTRACT

Plastic is used in many forms in day-to-day life. Since plastic is non-biodegradable, landfills do not provide an environment friendly solution. Hence, there is strong need to utilize waste plastic. This creates a large quantity of garbage every day which is unhealthy and pollutes the environment. In present scenario solid waste management is a challenge in our country. The production of solid waste is increasing day to day and causes serious concerns to the environment. In this study, the recycled plastics are used in the concrete as a partial replacement of fine aggregate in concrete. The main purpose of this study is to investigate the mechanical properties of concrete such as workability, compressive, flexural and split tensile strengths of concrete mixes with partial replacement of conventional fine aggregate with aggregate produced from plastic waste. The use of plastic aggregate as replacement for fine aggregate enhances workability and fresh bulk density of concrete mixes. The mechanical properties of concrete such as compressive, flexural, and tensile strengths of concrete reduced marginally up to 10% replacement levels..

1. Introduction

There are about 15342 tons of plastic waste produced in India every day, only 9205 tons recycled and dumped onto the soil^[1]. Environmental sustainable development is one of the most important problems facing the world today. The use of plastic is quickly growing for different reasons worldwide. It can have damaging impacts because of the use of chemical additives in plastic production. This plastic waste must therefore be monitored or recycled. Plastic bags are not degradable and take 1000 years to

degrade, causing groundwater contamination. It produces issues such as soil, water and air pollution because of the non-degradation property of plastics. Thus, these materials can be used suitably in other sectors to decrease these effects on the environment^[2]. Concrete is one of the most common and widely used construction materials in the world^[3]. Concrete industry conducts numerous tests for using such waste^[4] to decrease environmental burdens. The use of various types of solid waste as building material may decrease the demand for natural raw materials. This reduces the demand for natural resources to achieve sustainable development by using plastic waste

**Corresponding Author:*

Sudarshan D. Kore,

School of Construction Management, National Institute of Construction Management and Research (NICMAR), Balewadi, Pune, India

Email: sudarshankore123@gmail.com, skore@nicmar.ac.in

in concrete mixtures.

1.1 Generation of Plastic Waste

Approximately 6.3 billion tonnes of plastic waste was produced worldwide in 2016, while the amount of plastic waste produced in India amounts to 15.342 tonnes everyday.



Figure 1.1 Dumping of Plastic Waste in Open Lands

1.1.1 State of Art

The investigation of concrete combinations with the use of plastic waste to replace fines in several percentages, 10%, 20%, 30% and 40% by Ghernouti, Rahebi, Safi, & Chaid (2009) in their investigation^[5]. There has been an increase in workability because the plastic waste has nonabsorbent property. There have been significant reductions in flexural and compressive strength. The volume of void in concrete rises by plastic waste, which reduces the concrete's compactness.

Ismail & Al-Hashimi (2010)^[6] reported the addition of polymeric material leads to the formation of polymer film during hydration resulting in co-matrix during which polymer is amalgamated with cement hydrate^[7]. Another study by Raghatare (2012) revealed a decrease in mechanical properties by incorporating plastic as fine aggregate into concrete^[8]. But mechanical properties decreased by 10% and according to BIS 456 (2000)^[9], this is acceptable. The findings achieved by earlier scientists have been contradicted by Mathew et al., (2013)^[10].

Khilesh (2014) in his study, reports that the use of plastic waste together with the addition of steel fiber into concrete enhances the mechanical properties of concrete^[11].

The substitution of natural ground aggregate with plastic aggregates improves the concrete compressive strength by roughly 10 per cent relative to control concrete, at a replacement of 20 per cent. Chen et al. (2015) recorded the observation of only a 15 percent loss of strength at 10 percent replacement level, whereas a remarkable decrease was noted at another replacement level^[12]. It also has been indicated that the HDPE is able to limit the formation of cracks due to the increase in tensile strength. Mashaly et al. (2015) indicated that replacing 10% coarse aggregate from plastic wastes in concrete marginally lowered workability and dry density^[13]. The concrete that has been modified using plastic waste as fine aggregates (1% 3% and 5% by weight) reduces the mechanical characteristics of the concrete marginally and that reduction of 10% is acceptable^[14].

The substitution of sand by plastic waste (10%, 15% and 20%) decreased the working ability of mixed concrete by uneven size and overall shape, which lowered the fluidity^[15]. The hydrophobic property of the plastic reduces the hydration process, which reduces the mechanical strengths of concrete mixtures.

Studies by previous researchers have shown that the use of plastic wastes as a good aggregate in concrete blends has no adverse effect. The present study focuses on the use of fine aggregates produced from the crushing of solid plastic waste in concrete mixes as replacement 5%, 10%, 15%, 20% and 25% by weight for conventional fine aggregate. The mechanical characteristics of concrete are assessed, including working ability, compressive strength, split tensile strength and flexural strength.

2. Material Characterization

In this research the cement used meets the limitation of BIS 1489 Part 1-1991 (1991)^[16]. Table 2 shows the physical characteristics assessed in the laboratory.

Table 2.1 Properties of Cement

Initial setting time	30 min.
Final setting time	610 min.
Compressive strength	
3 day	28 N/mm ²
7 day	37 N/mm ²
28 day	59 N/mm ²
Consistency	28 %
Specific gravity	3.14

The fine and coarse aggregate confirms the BIS: 383-1960 (1997)^[17]. The physical characteristics of aggregates

are listed below in Table 2.2. Figure 2.1 shows the gradation of aggregates.

Table 2.2 Properties of Aggregates

Sr. No	Property	Natural Sand	Plastic Aggregate	Natural Coarse Aggregate
1	Specific gravity	2.73	-	2.90
2	Water absorption (%) by weight	1.62	Nil	0.60
3	Grading Zone	Zone II As per Table 4 of BIS 383	Zone II As per Table 4 of BIS 383	As per Table 2 of BIS 383

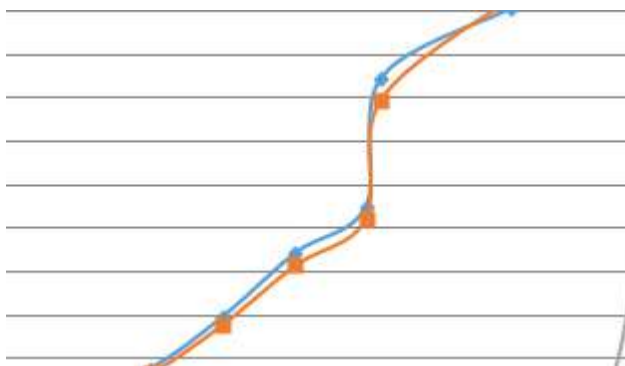


Figure 2.1 Gradation of Aggregates



Figure 2.2 Production of Aggregate from Plastic Waste

The plastic waste aggregate is of a variety of sizes. The particle size ranges between 0.15 mm and 12 mm in length and between 0.15 and 4 mm in thickness. Table 2.2 shows the physical characteristics of the plastic aggregate, and Figure 2.2 shows the manufacturing method.

3. Methodology

3.1 Mix Proportioning

The concrete M20 mixture is designed with a water-cement ratio of 0.55 in accordance with the BIS 10262:2009 (1999)^[18]. All the ingredients were mixed dry for 3 minutes and added water to obtain the homogeneous mixture. The sand has been substituted by a plastic

aggregate of 5%, 10%, 15%, 20% and 25% at separate levels. Table 3.1 shows the mix proportions.

Table 3.1 Mix Proportion

Mix code	Water (lit/m ³)	Cement (kg/m ³)	Natural sand (kg/m ³)	Plastic aggregate (kg/m ³)	Natural Coarse Aggregate (kg/m ³)
C0	197	394	703	0	1219
C5	197	394	668	35	1219
C10	197	394	633	70	1219
C15	197	394	598	106	1219
C20	197	394	563	141	1219
C25	197	394	528	176	1219

Note:

C0 - Shows reference mix designed as per BIS 10262-2009

C5, C10, C15, C20, C25 - Shows concrete mix containing 5%, 10%, 15%, 20%, 25% plastic waste as fine aggregate respectively.

3.2 Experimental Program

The cubes of 150 mm × 150 mm × 150 mm and beams of 600 mm × 150 mm × 150 mm were cast as per BIS: 516 (1959) for compressive and flexural strength determination^[19]. For the determination of Split Tensile Strength of concrete the specimens of size 300 mm × 150 mm were used. All samples were held aside at room temperature after casting, 24 hours later. BIS 1199 (1959) used evaluate concrete workability^[19]. The compressive and flexural strengths of concrete samples were calculated at the age of 7 and 28 days as per BIS: 516-1959 (2002)^[20]. At the age of 7 and 28 days of curing the compressive and Flexural strengths of concrete specimens were determined as per BIS: 516-1959 (2002)^[20].

4. Result and Discussion

4.1 Workability Test

The freshly prepared concrete mix was used to measure the workability of concrete by using slump test and results were presented in Figure 4.1.

Mix code	Water (lit/m ³)	Cement (kg/m ³)	Natural Sand (kg/m ³)	Plastic Aggregate (kg/m ³)	Natural Coarse Aggregate (kg/m ³)
C0	197	394	703	0	1219
C5	197	394	668	35	1219
C10	197	394	633	70	1219
C15	197	394	598	106	1219
C20	197	394	563	141	1219
C25	197	394	528	176	1219

Figure 4.1 Workability of Concrete Mixes

Results of the slump cone test showed the working ability of the plastic aggregate substitution to be increased considerably. The working ability of concrete mixes was improved by roughly 12%, by 15%, 19%, 26% and 33%, respectively, in relation to C5, C10, C15, C20 and C25. Due to the incorporation of plastic waste into concrete, a soft surface and plenty of open water led to enhanced working capacity. The plastic aggregate does not absorb water, so the followability of concrete can also be increased.

4.2 Density

The fresh wet densities of all the concrete mixtures are presented in Figure 4.2.

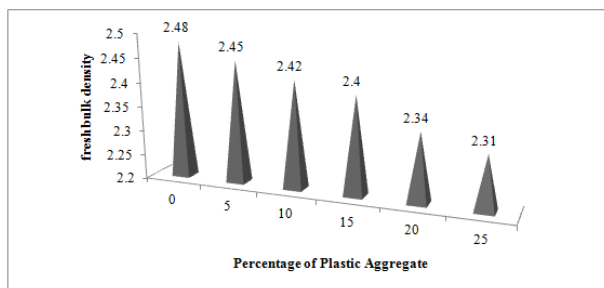


Figure 4.2 Density of Concrete Mixtures

The finding shows that, the fresh density tends to decline by 1.20%, 2.42%, 3.2%, 5.6% and 6.8% at 5%, 10%, 15%, 20% and 25% respectively to that of reference mixture. The density of concrete is mostly governed by the densities of the ingredients used in the blend. This is helpful in lightweight concrete manufacturing because of the low density of plastic waste as compared to sand.

4.3 Compressive Strength

Figure 4.3 presents the compression strength of concrete made using plastic waste as a fine aggregate. The compressive strength is determined at 7 and 28 days and compared with the reference mixtures.

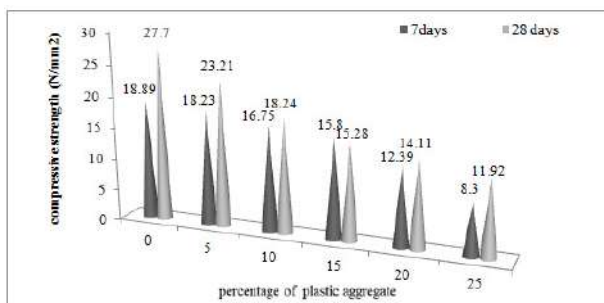


Figure 4.3 Compressive Strength of Concrete Mixtures

In all the concrete mixtures made with plastic aggregates, the significant reduction was observed. At 7 days, the compressive strength decreased from 3% to 56%

at 28 days it approximately decreased from 16% to 57% at 5% to 25% replacement ratios respectively relative to that of reference blend. This reduction was probably caused by the poor adhesive strength in the concrete blends between the plastic aggregate layer and the cement paste.

4.4 Flexural Strength

The difference in flexural strength of all concrete mixes for 7 days and 28 days are shown in Figure 4.4.

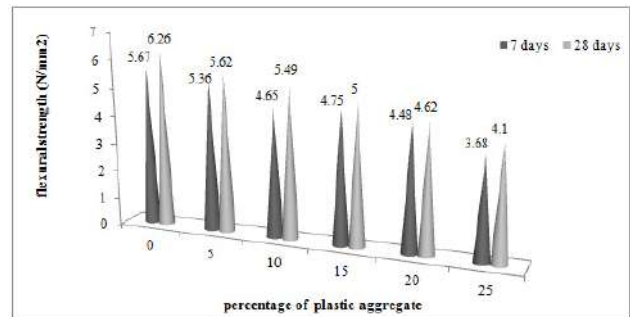


Figure 4.4 Flexural Strength of Concrete Mixtures

The flexural strength of concrete prepared with plastic aggregate gradually decreased. The 7-day flexural strength of concrete mixture with plastic aggregate reduced from 5% to 35%, at 28 days it reduced by 10% to 35% at replacement levels of 5% to 25% respectively. This decline was due to the low cohesive bond between the plastic aggregate and cement paste. Also, plastic aggregates are of hydrophobic nature which restricts cement hydration resulting in a loss in strength.

4.5 Split Tensile Strength

The results obtained in the laboratory testing of split tensile strength are shown in Figure 4.5.

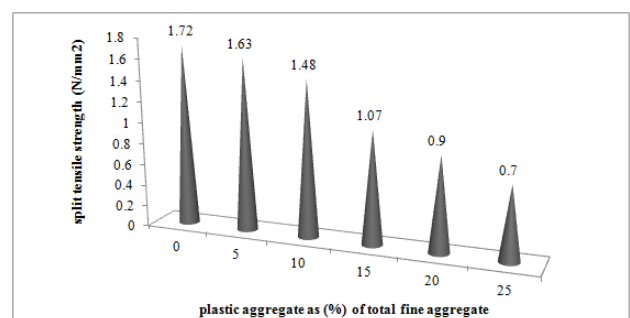


Figure 4.5 Split Tensile Strength of Concrete Mixtures

The findings showed that the split tensile strength of waste plastic concrete mixtures at each curing age is prone to decrease with the replacement of plastic aggregate. The split tensile strength of concrete produced with plastic aggregate decreased by roughly 5% to 50% at replacement rates of 5% to 25% as concerning that of reference blend. The findings of this test are consistent

with the compressive strength test.

5. Conclusion

An investigation was conducted to examine the mechanical characteristics of plastic-modified concrete as a substitute for natural sand and was noted that,

- There was an increase in slump values in concrete blends generated by plastic aggregates. In order to decrease the water-cement ratio, excess water would be used.

- The compressive strength of the prefabricated concrete mixture was significantly reduced as the substitution percentage increased.

- Flexural and split tensile strength findings are as in the compressive strength test line.

The concrete produced was generally appropriate in mechanical characteristics for the use of this plastic waste. A more thorough research is needed to preserve the mechanical characteristics of concrete mixtures made as a whole with plastic waste. This means that the issue of landfill and dumping can be substantially decreased by using such waste in concrete.

References

- [1] United Nations Environment Programme. (2009). *Converting Waste Plastics into a Resource- Assessment Guidelines*. Retrieved from <http://wedocs.unep.org/handle/20.500.11822/7864>.
- [2] Hassani, A.A., Ganjidoust, A., Maghanaki, H. (2005). Use of Plastic Waste (Poly-ethylene Terephthalate) in Asphalt Concrete Mixture as Aggregate Replacement., *Waste Manag. Res.* 23, 322–327. DOI: 10.1177/0734242X050506739.
- [3] Kore, S. D., Vyas, A. K. (2017). Impact of Fire on Mechanical Properties of Concrete Containing Marble Waste. *Journal of King Saud University – Engineering Sciences*. DOI: 10.1016/j.jksues.2017.03.007.
- [4] Kore, S. D., Vyas, A. K. (2016). Impact of Marble Waste as Coarse Aggregate on Properties of Lean Cement Concrete. *Case Studies in Construction Materials*, Vol. 4, pgs. 85–92. DOI:10.1016/j.cscm.2016.01.002.
- [5] Ghernouti, Y., Rabehi, B., Safi, B., & Chaid, R. (2009). Use of Recycled Plastic Bag Waste in the Concrete. *Journal of International Scientific Publications: Materials, Methods and Technologies*, Vol. 8, pgs. 480–487.
- [6] Ismail, Z. Z. & Al-Hashmi, E. (2010). Validation of Using Mixed Iron and Plastic Wastes in Concrete. *Second International Conference on Sustainable Construction Materials and Technologies* June 28- June 30, 2010.
- [7] Dionys, V. G., Czarnecki, L., Maultzsch, M., Schorn, H., Beeldens, A., Lukowski, P., & Knapen, E. (2005). *Cement Concrete and Concrete-Polymer Composites: Two Merging Worlds: A Report from 11th ICPC Congress in Berlin, 2004*, *Cement and Concrete Composites*, Vol. 27 (9-10), pgs. 926-933.
- [8] Raghatate Atul M. (2012), Use of Plastic in a Concrete to Improve its Properties. *International Journal of Advanced Engineering Research and Studies*, pgs. 109–111.
- [9] Bureau of Indian Standards (2000), *Plain and Reinforced Concrete - Code of Practice*, IS 456-2000, New Delhi, India.
- [10] Mathew, P., Varghese, S., Paul, T., & Varghese, E. (2013). Recycled Plastics as Coarse Aggregate for Structural Concrete. *International Journal of Innovative Research in Science, Engineering and Technology*, Vol. 2 , pgs. 687–690.
- [11] Khilesh , S. (2014). Study of Strength Property of Concrete Using Waste Plastics and Steel Fiber. *The International Journal of Engineering and Science (IJES)*, pgs. 9–11.
- [12] Chen, C. C., Jaffe, N., Koppitz, M., Weimer, W., & Polocoser, A. (2015). Concrete Mixture with Plastic as Fine Aggregate Replacement. *International Journal of Advances in Mechanical and Civil Engineering*, Vol. 2. Pgs. 49-53.
- [13] Mashaly, A. O., El-Kaliouby, B. A., Shalaby, B. N., El-Gohary, A. M., & Rashwan, M. A. (2015). Effects of Marble Sludge Incorporation on the Properties of Cement Composites and Concrete Paving Blocks. *Journal of Cleaner Production*, Vol. 112, pgs. 731-741. DOI: <https://doi.org/10.1016/j.jclepro.2015.07.023>
- [14] Jibrael, M. A., Peter, F. (2016). Strength and Behavior of Concrete Contains Waste Plastic. *Journal of Ecosystem & Ecography*, Vol. 6, 186. DOI: 10.4172/2157-7625.1000186
- [15] Ismail, Z. Z., & Al-Hashmi, E. A. (2017). Use of Waste Plastic in Concrete Mixture as Aggregate Replacement. *Waste Management*, Vol. 28(11), pgs. 2041-2047. DOI: <https://doi.org/10.1016/j.wasman.2007.08.023>
- [16] Bureau of Indian Standards (1991). *Specification for Portland Pozzolana Cement*. BIS:1489 (Part-1) 1991, New Delhi, India.
- [17] Bureau of Indian Standards (1997). *Specification for Coarse and Fine Aggregates from Natural Sources for Concrete*. BIS:383, New Delhi, India; 1970.
- [18] Bureau of Indian Standards (1999). *Recommended Guidelines for Concrete Mix Design* IS:10262-

- 1982, New Delhi, India.
- [19] Bureau of Indian Standards (1959). Indian standard Methods of Sampling and Analysis of Concrete, New Delhi, India.
- [20] Bureau of Indian Standards (2002). Specification for Methods of Tests for Strength of Concrete BIS:516-1959, New Delhi, India.

ARTICLE

Significance of Stone Waste in Strength Improvement of Soil

Amit Kumar^{1*} Kiran Devi¹ Maninder Singh¹ Dharmender Kumar Soni¹

Civil Engineering Department, National Institute of Technology, Kurukshetra, India 136119.

ARTICLE INFO

Article history

Received: 20 September 2019

Accepted: 20 November 2019

Published:

Keywords:

Stabilization

Stone waste

Maximum dry density

Optimum moisture content

Unconfined compressive strength

Linear regression equation

ABSTRACT

The evolution of industries is essential for the economic growth of any country; however, this growth often comes with exploitation of natural resources and generation of wastes. The safe disposal and utilisation of industrial wastes has become essential for sustainable development. A possible approach would be to utilize these wastes in construction industries. The stone industry is one such flawed industries that generates waste in dust or slurry form; this leads harmful impacts on human beings, animals, and surrounding areas which, in turn, can lead to soil infertility. In the present study, stone waste was examined for its influence on maximum dry density (MDD), optimum water content (OMC) and unconfined compressive strength (UCS) of soil experimentally. Stone waste was used at 0%, 4%, 8%, 12%, 16% and 20% by weight of soil and UCS tests were conducted at maturing periods of 7, 14 and 21 days. Test results reported that the incorporation of stone waste improved the compressive strength value significantly. Maximum dry density was enhanced; however, optimum water content was reduced with the use of stone waste in soil due to its fine particles. Linear regression equations were also derived for various properties.

1. Introduction

Industrialization promotes the generation of industrial by-products along with the usable final products. These wastes may be in solid, liquid and gaseous form. Nowadays, finished stone is an important building material used at various parts of a household. The stones generally are of different types, such as granite, marble, limestone, Kota stone etc. The stone can be used in the construction following a dimensioning process, which makes it more suitable for use as required. During the cutting and polishing process of stone blocks, a continuous stream of water is sent over the saw-blade to cool down the machine. The waste water, along with very fine particles of stone, comes out as slurry, which is

dumped into surrounding area.

Within the overall production of stone waste of approximately 80 lakh metric tonne (MT) per year, about 12 lakh MT is produced as fine dust waste, and from which 4-5 lakh MT is disposed nearby mine sites, and rest of them disposed directly to the lands and water courses.

Safe disposal of the industrial wastes has become a serious threat to humans. Direct disposal of wastes to the land or water courses is not a mere nuisance; it also unbalancing the ecosystem. Stone industry also produces waste in the form of block pieces, slurry or dust that originates during the dimensioning of stones. The waste produced from the stone industry is non-biodegradable and direct dumping in open land may cause soil infertility

*Corresponding Author:

Amit Kumar,

Civil Engineering Department, National Institute of Technology, Kurukshetra, India 136119.

Email: kauleamit0089@gmail.com

by clogging the soil pores. If this waste contaminates water sources, flora and fauna dependent on these water sources may experience other serious problems and even death. Dry stone powder is very dangerous to both humans and animals, as its direct exposure may give rise to respiratory problems, eye and throat diseases too. Considering its severity, a safe and manageable disposal is needed^[1]. Road construction industries may utilise the stone waste as a raw material or soil stabiliser. As the stone waste is available free of cost, weak geological formation may be stabilised by using stone waste. In the past, many investigators have used the stone waste as an additive or stabiliser for weak soil and found better results against loading and weathering conditions. Replacing the marble powder in marble bricks with Kota stone powder improved the compressive strength^[2]. Intrusion of Kota stone in clayey subgrade has shown appreciable changes in California Bearing Ratio (CBR) value and compressibility characteristics^[3]. Stone slurry waste was also found effective for soil stabilisation in terms of compaction, strength and CBR properties of soil^[4]. Improvements in soil properties were also observed in highly compressible soil like black cotton soil (BCS) with other additives such as sawdust and fibres. The improvement was noted from 26% to 35% and higher content of fibres may reduce the dry density of soil due to its low density as compared to soil^{[5][6]}. Replacing marble slurry with Kota stone sludge revealed better results^[7]. Kota stone slurry was found to be a good stabiliser for BCS subgrade. The treated soil showed remarkable changes in UCS and CBR values^[8]. Calcium-based additive i.e. eggshell powder was found as a good waste material to improve the strength characteristics of silty soil, as observed through physicochemical tests^[9].

In the present study, stone waste was used to improve the compaction and strength characteristics of a clayey soil. As the stone waste mainly contains calcium content, so it may be effective for the treatment of clayey soil. In addition, utilization of stone waste in the soil stabilization reduces its disposal-related problem and other associated issues. For the rationalisation of the results, linear regression equations were also utilised. The objective of study was to utilize stone waste in soil to minimize its consequences to the ecosystem, along with improvement in soil properties.

2. Materials and Methodology

To realize the objectives, the whole procedure commenced in two phases. The first phase comprised of the determination of MDD and OMC of parent and treated soil using standard proctor test method as per IS: 2720 (VII) 1974, and strength test by performing unconfined

strength test referring IS: 2720 (X) 1991^{[10][11]}. During the second phase, analysis of results was done to generate linear regression equations for the compaction and strength parameters.

2.1 Materials

The soil was procured from the potholes of a construction site at Kurukshetra, India. Before digging the potholes, the vegetation must be peeled off to avoid all alien objects. Indian Standard Classification System (ISC) confirmed the subjected soil as the CL type according to plasticity chart method and other necessary index properties of soil (tabulated in Table 1). Granulometric curve of the soil is shown in Figure 1. Stone slurry, a waste material obtained from Kota stone, from Rajasthan, India, generated during the processing of stones, was dried and grinded to powder to use as an additive. The stone powder was sieved through a 425 μ m sieve before use. The idea behind sieving was to maintain the uniformity of the size of material. Usually, stone waste is white in color, with chemical properties as per Table 2. The scanning electron micrograph and energy dispersive X-ray spectrogram of stone waste are shown in Figures 2a and 2b^[12]. The laboratory's available tap water supply was used during whole course of experimentation.



Figure 1. Grain Size Distribution Curve of Soil

Table 1. Properties of Soil

Physical Parameter	Value
Liquid limit	29%
Plastic limit	20%
Plasticity index	9%
Soil type	CL
γ_d max	1.72g/cc
OMC	14.5%

Table 2. Typical Chemical Composition of Stone Waste

Chemical Constituent	Chemical Composition (%)
Calcium oxide	49.78
Silica	17.01
Aluminium Oxide	2.92
Magnesium oxide	0.61

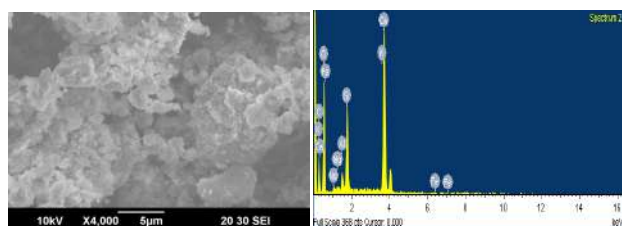


Figure 2a. SEM of SSP Figure 2b. EDS of SSP

1.2 Test Procedure

2.2.1 Standard Proctor Test

A series of tests was conducted to determine OMC and MDD of parent and treated soil, confirming to IS: 2720-1974 (Part VII)^[10]. Stone waste was taken by dry weight of soil, and was mixed and dried during whole testing. After every layer of soil was scratched with a brush to improve its bond with the proceeding layer, the proctor mould was filled up to the attached collar in 3 layers using the lightweight compaction procedure. The stone waste was used at different percentages. The designated mixes have been given in Table 3.

Table 3. Mix Designation for Experimentation

Mix Number	Stone waste (%)
S1	0
S2	4
S3	8
S4	12
S5	16
S6	20

1.1.2 Unconfined Compressive Strength

The samples were prepared in the cylindrical mould confirming to IS: 2720-1991 (Part X)^[11]. The wet homogenous mixture was placed inside the specimen mould in seven layers using a spoon, levelled and gently tap-compacted by 1cm diameter mild steel ram. The sample was kept under static load for at least 10 minutes in order to account for any deformation occurring due to moisture change. The sample was then removed from the mould with the help of the sample extruder and measured for its dimension. To maintain the consistency of the sampling, each sample was prepared for 38 mm diameter and 76 mm in length. To maintain the repeatability of the results, samples were prepared in triplicity and mean of the results of each sample was taken for the calculation.

2.2.3 Statistical Analysis

After performing the laboratory tests, the results were analyzed to create linear regression equations.

3. Results and Discussion

3.1 Optimum Moisture Content and Maximum Dry Density

The consequences of stone waste on maximum dry density and optimum moisture content were investigated experimentally, and results of MDD and OMC have been shown in Figures 3a and 3b respectively. Figure 3a showed that the increase in stone waste content in soil enhanced the maximum dry density. The increase in MDD may be due to finer particles of the stone waste.

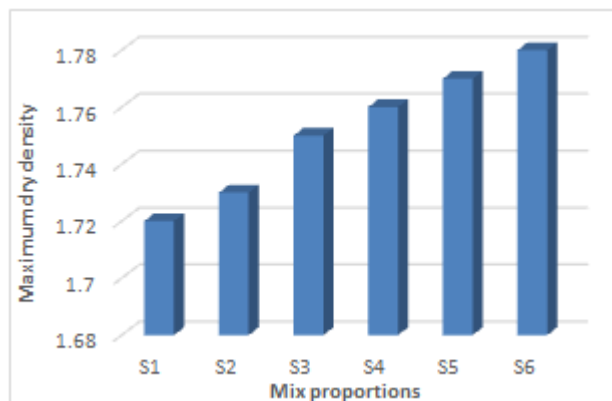


Figure 3a. Variation in MDD

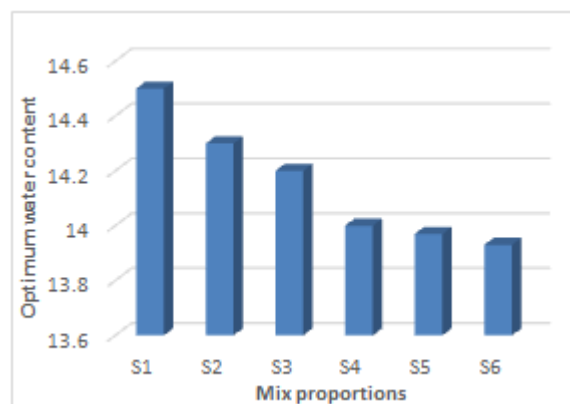


Figure 3b. Variation in OMC of Soil Using Stone Waste

The use of stone waste in soil had reduced the moisture content as shown in Figure 3b. The very fine particles of stone waste were responsible for the reduction in moisture content of soil. The similar trend of MDD and OMC was also observed in other related studies^{[13][14]}.

Figures 3a and 3b also show that stone waste increased the dry density. The increase in dry density was 0.58% to 3.49% as compared to the parent soil. A possible reason for the improvement in maximum dry density upon the inclusion of stone waste is the fineness of stone waste that fills the voids of the soil and helps to create a denser material. A decrease in optimum moisture content was also observed. Stone waste contains an appreciable amount of lime. As long as lime present in the mix, more water is required to react. As a result, this reaction, known as the pozzolanic reaction, results in the greater consumption of

water in the mix.

3.2 Unconfined Compressive Strength

Figure 4 shows the effect of stone waste on the unconfined compressive strength (UCS) of the soil at various curing ages i.e. 7, 14 and 21 days. From Figure 4, it has been observed that UCS varied proportionally to increases in stone waste percent and curing ages. The enhancement in UCS may be due to addition of fine particles of stone waste. The maximum strength gain was obtained at 20% intrusion of stone waste for all the curing ages. The similar results also reported in related studies^[15].

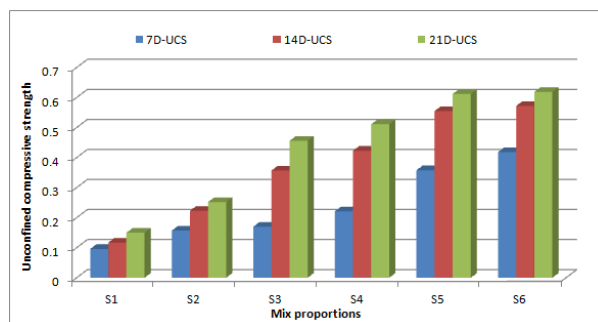


Figure 4. Variation of UCS at Varied Curing Age

Stone waste increased the UCS linearly and was found to be very effective in increasing the UCS of the subjected soil. The percentage increase in UCS varied from 0.58% to 3.49% after inclusion of stone waste from 4% to 20%.

3.3. Regression Analysis

To check the rationalization of the presented study, a regression analysis of the responses was also carried out. Linear regression analysis of MDD, OMC and UCS was done and has been shown in Figures 5a, 5b and 5c respectively.

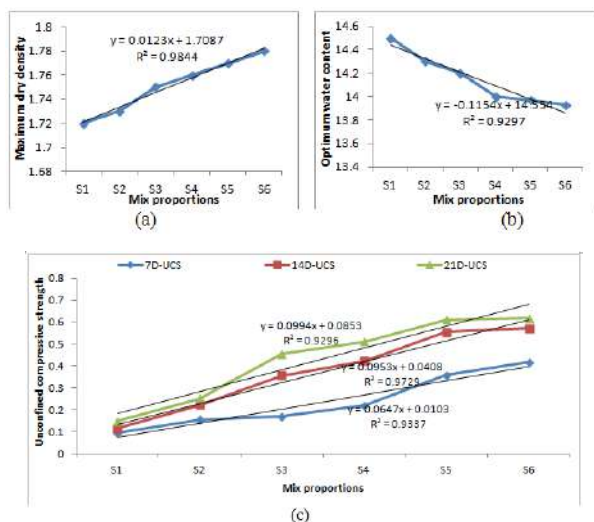


Figure 5. Regression Analysis for (a) MDD; (b) OMC; and (c) UCS at 7, 14 and 21 Days

From Figures 5 (a), (b) and (c), it can be seen that regression equations showed good results in terms of R-squared i.e. near to unity. As such, these regression equations can be used in future to predict the compaction and strength characteristics of such type of low compressible soils.

4. Conclusion

Present study represents the occurrence of stone waste inclusion in plastic soil. Stone waste was introduced in soil at varied percentages and the effect on compaction and strength characteristics was researched. For viability of the results, regression equations were also obtained using responses of the experiments under laboratory conditions. The following conclusions can be drawn from the present study:

1. Maximum dry density increased and optimum moisture content decreased linearly with the increase in stone waste.
2. Fine particles of stone waste filled the voids and helped to increase the dry density of soil.
3. Available calcium of stone waste reacted with clay minerals and started pozzolanic reaction, which helped for the attainment of long-term strength.
4. Linear regression equations showed reliability of the results.

In the present study, utilisation of stone waste in soil works resulted in improvement of soil parameters. So, freely available stone waste can be utilized to stabilize the subgrade of pavement and make it cheaper for practitioners and engineers. As a wise step to make environment safe and eco-friendly always appreciated.

References

1. Devi, K., Saini, B., & Aggarwal, P. (2019). Combined Use of Accelerators and Stone Slurry Powder in Cement Mortar. *ICSWMD 2019*, LNCE 21:1-8. DOI: https://doi.org/10.1007/978-3-030-02707-0_25.
2. Mehta, J., & Pitroda, J. K. (2016). Experimental Investigation for the Kota Stone Powder as Replacement of Marble Powder in Marble Brick. *International Journal of Current Trends in Engineering & Research (IJCTER)*, 2(4):105 – 111.
3. Ola, M., & Goyal, S. (2016). Improvement of Clayey Subgrade by Adding Kota Stone: A Review. *International Journal of Technical Research (IJTR)*, 5(1):147-149.
4. Saini, Y., & Soni, D. K. (2017). Stabilization of Clayey Soil by Using Stone Slurry Waste and Cement: Review. *International Journal of Advanced Technology in Engineering and Science*, 5(1):343-349.
5. Jangid, A. K., Khatti, J., & Bindlish, A. (2018).

- Stabilization of Black Cotton Soil by 15% Kota Stone Slurry with Wooden Saw Dust. *International Journal of Advance Research in Science and Engineering*, 7(2):108-114.
6. Jangid, A.K., Khatti, J., & Bindlish, A. (2018). Stabilization of Black Cotton Soil by 15% Kota Stone Slurry with Recron 3s Fibre. *International Journal of Advance Research in Science and Engineering*, 7(2):102-107.
 7. Singh, V., Verma, A., & Chaurasiya, R.P. (2018). Study Paper on Stabilization of Black Cotton Soil with Kota Stone Sludge Replacement Marble Slurry. *National Journal of Multidisciplinary Research and Development*, 3(1):1053-1056.
 8. Rathore, A.P.S., & Parbhakar, K. (2018). Soil Stabilization Using Kota Stone Slurry in Pavement. *International Journal of Innovative Research in Science, Engineering and Technology*, 7(5):6147-6152.
 9. Kumar, A., & Soni, D.K. (2019). Significance of pH in Fine-grained Soil. *ICSWMD, LNCE 21 2019:1-9*. DOI: https://doi.org/10.1007/978-3-030-02707-0_32.
 10. IS: 2720 (Part 7)-1974. Indian Standard Methods of Test for Soils: Determination of Moisture Content-Dry Density Relation using Light Compaction, *Bureau of Indian Standards*, New Delhi, India.
 11. IS: 2720 (Part 10)-1991. Indian Standard Methods of Test for Soils: Determination of Unconfined Compressive Strength, *Bureau of Indian Standards*, New Delhi, India.
 12. Devi, K., Saini, B., & Aggarwal, P. (2019). Utilization of Kota Stone Slurry Powder and Accelerators in Concrete, *Computers and Concrete*, 23(3):189-201. DOI: <http://dx.doi.org/10.12989/cac.2019.23.3.189>
 13. Sivrikaya, O., Kiyıldı, K. R., & Karaca, Z. (2014). Recycling Waste from Natural Stone Processing Plants to Stabilise Clayey Soil. *Environmental Earth Science*, 71:4397-4407. DOI 10.1007/s12665-013-2833-x
 14. Ramadas, T. L., Kumar, N. D., & Aparna, G. (2010). Swelling and Strength Characteristics of Expansive Soil Treated with Stone Dust and Fly Ash. In: *Indian Geotechnical Conference*, GEO-trendz, Bombay, pp 557-560.
 15. Xiao, Z., & Xu, W. (2019). Assessment of Strength Development in Cemented Coastal Silt Admixed Granite Powder. *Construction and Building Materials*, 206:470-482. DOI: <https://doi.org/10.1016/j.conbuildmat.2019.01.231>

Author Guidelines

This document provides some guidelines to authors for submission in order to work towards a seamless submission process. While complete adherence to the following guidelines is not enforced, authors should note that following through with the guidelines will be helpful in expediting the copyediting and proofreading processes, and allow for improved readability during the review process.

I . Format

- Program: Microsoft Word (preferred)
- Font: Times New Roman
- Size: 12
- Style: Normal
- Paragraph: Justified
- Required Documents

II . Cover Letter

All articles should include a cover letter as a separate document.

The cover letter should include:

- Names and affiliation of author(s)

The corresponding author should be identified.

Eg. Department, University, Province/City/State, Postal Code, Country

- A brief description of the novelty and importance of the findings detailed in the paper

Declaration

v Conflict of Interest

Examples of conflicts of interest include (but are not limited to):

- Research grants
- Honoria
- Employment or consultation
- Project sponsors
- Author's position on advisory boards or board of directors/management relationships
- Multiple affiliation
- Other financial relationships/support
- Informed Consent

This section confirms that written consent was obtained from all participants prior to the study.

- Ethical Approval

Eg. The paper received the ethical approval of XXX Ethics Committee.

- Trial Registration

Eg. Name of Trial Registry: Trial Registration Number

- Contributorship

The role(s) that each author undertook should be reflected in this section. This section affirms that each credited author has had a significant contribution to the article.

1. Main Manuscript

2. Reference List

3. Supplementary Data/Information

Supplementary figures, small tables, text etc.

As supplementary data/information is not copyedited/proofread, kindly ensure that the section is free from errors, and is presented clearly.

III . Abstract

A general introduction to the research topic of the paper should be provided, along with a brief summary of its main results and implications. Kindly ensure the abstract is self-contained and remains readable to a wider audience. The abstract should also be kept to a maximum of 200 words.

Authors should also include 5-8 keywords after the abstract, separated by a semi-colon, avoiding the words already used in the title of the article.

Abstract and keywords should be reflected as font size 14.

IV . Title

The title should not exceed 50 words. Authors are encouraged to keep their titles succinct and relevant.

Titles should be reflected as font size 26, and in bold type.

IV . Section Headings

Section headings, sub-headings, and sub-subheadings should be differentiated by font size.

Section Headings: Font size 22, bold type

Sub-Headings: Font size 16, bold type

Sub-Subheadings: Font size 14, bold type

Main Manuscript Outline

V . Introduction

The introduction should highlight the significance of the research conducted, in particular, in relation to current state of research in the field. A clear research objective should be conveyed within a single sentence.

VI . Methodology/Methods

In this section, the methods used to obtain the results in the paper should be clearly elucidated. This allows readers to be able to replicate the study in the future. Authors should ensure that any references made to other research or experiments should be clearly cited.

VII . Results

In this section, the results of experiments conducted should be detailed. The results should not be discussed at length in

this section. Alternatively, Results and Discussion can also be combined to a single section.

VIII. Discussion

In this section, the results of the experiments conducted can be discussed in detail. Authors should discuss the direct and indirect implications of their findings, and also discuss if the results obtain reflect the current state of research in the field. Applications for the research should be discussed in this section. Suggestions for future research can also be discussed in this section.

IX. Conclusion

This section offers closure for the paper. An effective conclusion will need to sum up the principal findings of the papers, and its implications for further research.

X. References

References should be included as a separate page from the main manuscript. For parts of the manuscript that have referenced a particular source, a superscript (ie. [x]) should be included next to the referenced text.

[x] refers to the allocated number of the source under the Reference List (eg. [1], [2], [3])

In the References section, the corresponding source should be referenced as:

[x] Author(s). Article Title [Publication Type]. Journal Name, Vol. No., Issue No.: Page numbers. (DOI number)

XI. Glossary of Publication Type

J = Journal/Magazine

M = Monograph/Book

C = (Article) Collection

D = Dissertation/Thesis

P = Patent

S = Standards

N = Newspapers

R = Reports

Kindly note that the order of appearance of the referenced source should follow its order of appearance in the main manuscript.

Graphs, Figures, Tables, and Equations

Graphs, figures and tables should be labelled closely below it and aligned to the center. Each data presentation type should be labelled as Graph, Figure, or Table, and its sequence should be in running order, separate from each other.

Equations should be aligned to the left, and numbered with in running order with its number in parenthesis (aligned right).

XII. Others

Conflicts of interest, acknowledgements, and publication ethics should also be declared in the final version of the manuscript. Instructions have been provided as its counterpart under Cover Letter.



**BILINGUAL
PUBLISHING CO.**
Pioneer of Global Academics Since 1984

Journal of Building Material Science

Aims and Scope

Journal of Building Material Science provides an international platform for the development of innovative research in the field of building materials, and the journal is dedicated to the insightful investigation and innovative use of materials in building operations. *Journal of Building Material Science and Technology* publishes detailed case studies and review articles, as well as short communications and discussions.

The scope of *Journal of Building Material Science* includes, but is not restricted to, all types of building materials used in architecture and construction such as:

- Steel
- Composite materials
- Concrete
- Green building materials
- Innovative materials in construction and civil engineering

Bilingual Publishing Co. (BPC)

Tel:+65 65881289

E-mail:contact@bilpublishing.com

Website:www.bilpublishing.com

About the Publisher

Bilingual Publishing Co. (BPC) is an international publisher of online, open access and scholarly peer-reviewed journals covering a wide range of academic disciplines including science, technology, medicine, engineering, education and social science. Reflecting the latest research from a broad sweep of subjects, our content is accessible world-wide—both in print and online.

BPC aims to provide an analytics as well as platform for information exchange and discussion that help organizations and professionals in advancing society for the betterment of mankind. BPC hopes to be indexed by well-known databases in order to expand its reach to the science community, and eventually grow to be a reputable publisher recognized by scholars and researchers around the world.

BPC adopts the Open Journal Systems, see on ojs.bilpublishing.com

Database Inclusion



Asia & Pacific Science
Citation Index



Creative Commons



China National Knowledge
Infrastructure



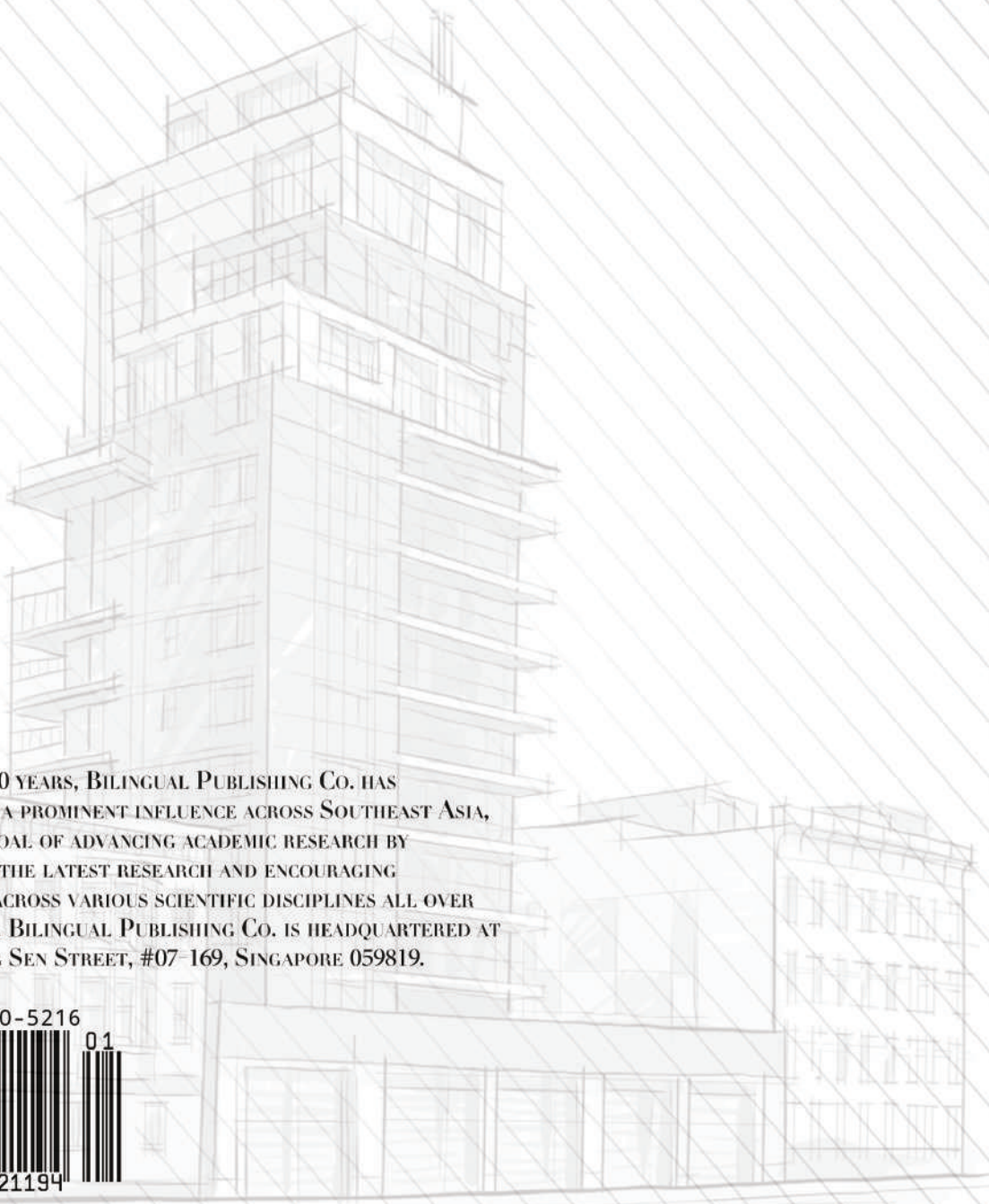
Google Scholar



Crossref



MyScienceWork



FOR OVER 30 YEARS, BILINGUAL PUBLISHING CO. HAS MAINTAINED A PROMINENT INFLUENCE ACROSS SOUTHEAST ASIA, WITH THE GOAL OF ADVANCING ACADEMIC RESEARCH BY PUBLISHING THE LATEST RESEARCH AND ENCOURAGING DISCOURSE ACROSS VARIOUS SCIENTIFIC DISCIPLINES ALL OVER THE WORLD. BILINGUAL PUBLISHING CO. IS HEADQUARTERED AT 12 EU TONG SEN STREET, #07-169, SINGAPORE 059819.

ISSN 2630-5216



9 772630 521194